Petroleum Research 11 (2026) 471–500

Contents lists available at ScienceDirect

Petroleum Research

journal homepage: http://www.keaipublishing.com/en/journals/petroleum-research/

Review Article

A review on cementing system for CO_2 storage wells: Mechanisms, testing protocols and screening criteria

Muhammad Hammad Rasool [a,b,c,*], Syahrir Ridha [a,b,**], Raja Rajeswary Suppiah [a,b,***], Suhaib Umer Ilyas [d], Shwetank Krishna [e], Muhammad Galang Mardeka [f], Muhammad Adeem Abbas [g], Husnain Ali [h]

[a] Institute of Sustainable Energy and Resources, Universiti Teknologi PETRONAS, Bandar Seri Iskandar, 32610, Malaysia
[b] Petroleum Engineering Department, Universiti Teknologi PETRONAS, Bandar Seri Iskandar, 32610, Malaysia
[c] Petroleum Geosciences Department, Universiti Teknologi PETRONAS, Bandar Seri Iskandar, 32610, Malaysia
[d] Chemical Engineering Department, University of Jeddah, Saudi Arabia
[e] Department Geoenergy, Montanuniversität Leoben, Parkstraße 27, 8700 Leoben, Austria
[f] Department of Petroleum Engineering, Institut Teknologi Bandung, 40116, Indonesia
[g] School of Petroleum Engineering, University of New South Wales, NSW 2052 Sydney, Australia
[h] Department of Chemical and Biological Engineering. Hong Kong Univeristy of Science and Technology, Hong Kong, China

ARTICLE INFO

Article history:
Received 8 July 2025
Received in revised form
16 October 2025
Accepted 16 October 2025
Available online 24 October 2025

Keywords:
CO_2 storage
Wellbore cementing
Acid-resistant cement
Calcium aluminate phosphate cement

ABSTRACT

Long-term containment of CO_2 in geological formations demands cementing systems that can withstand highly aggressive downhole environments, where carbonic acid, brine, and other reactive species threaten the integrity of cement sheath. This review critically examines the deterioration mechanisms of Portland-based cements under CO_2-rich conditions, emphasizing acid-induced decalcification, carbonation, and leaching processes. It further categorizes and compares a broad range of acid-resistant alternatives including modified Portland systems, non-Portland systems (CAC: Calcium Aluminate Cement, CAPC: Calcium Aluminate Phosphate Cement, MPC: Magnesium Phosphate Cement, geopolymers), resin-based sealants, and nano-engineered formulations, focusing on their chemistry, resistance mechanisms, performance metrics, and field applicability. The review then proposes a detailed laboratory testing system aligned with API standards and introduces a phase-wise testing protocol. A novel conceptual screening criterion (HSR framework) is developed based on operational, design, and sustainability parameters to guide material selection and validation for CO_2-brine exposed cementing systems. Among the systems evaluated, CAC, CAPC, and MPC have shown superior results in terms of post-exposure compressive strength retention and reduced carbonation depth. Key knowledge gaps and challenges are identified, particularly regarding long-term behavior under thermobaric and acidic exposure. Finally, a future roadmap is outlined, calling for systematic field validation, deeper mechanistic insights into CAC and CAPC systems, and innovations in multifunctional, low-carbon binders suited for emerging CCS frontiers.

1. Introduction

Carbon Capture and Storage (CCS) has emerged as a pivotal technology in the fight against climate change, designed to mitigate CO_2 emissions from industrial sources by permanently sequestering the gas in deep geological formations (Rasool and Ahmad, 2023; Rasool et al., 2023a,b; Tomić et al., 2018). Central to the long-term success of any CCS project is the structural

* Corresponding author. Institute of Sustainable Energy and Resources, Universiti Teknologi PETRONAS, Bandar Seri Iskandar, 32610, Malaysia.
** Corresponding author. Institute of Sustainable Energy and Resources, Universiti Teknologi PETRONAS, Bandar Seri Iskandar, 32610, Malaysia
*** Corresponding author. Petroleum Engineering Department, Universiti Teknologi PETRONAS, Bandar Seri Iskandar, 32610, Malaysia
E-mail addresses: hammad.rasool@utp.edu.my (M.H. Rasool), syahrir.ridha@utp.edu.my (S. Ridha), rajarajeswary@utp.edu.my (R.R. Suppiah).
Peer review under the responsibility of Editorial Office of Petroleum Research.

https://doi.org/10.1016/j.ptlrs.2025.10.001

integrity of the wellbore often the only engineered barrier between supercritical CO_2 and overlying groundwater resources or the atmosphere (Bai et al., 2016; Carey, 2013; Recasens et al., 2017). Once a site transitions from injection to post-operational monitoring, the cement sheath that lines the casing becomes the last line of defense against leakage (Zhang and Bachu, 2011). This critical function demands that cement systems must not only withstand extreme subsurface conditions often exceeding 100 °C in temperature and reaching pressures up to 30 MPa in deep saline aquifers but also resist continuous exposure to chemically aggressive environments created by the reaction of CO_2 with formation brines (Haagsma et al., 2017; Takase et al., 2010; Udebhulu et al., 2024). The CO_2 can leak through cement sheath in various scenarios as depicted in Fig. 1.

When CO_2 is injected into a subsurface formation, it rapidly dissolves into the native brine, forming carbonic acid (H_2CO_3). Under geochemical conditions typical of CCS reservoirs, this acid can lower the pH of the surrounding fluid to values between 3 and 4.5, triggering dissolution of key hydration phases in conventional Class G Portland cement (See Fig. 2) (Lesti et al., 2013; Udebhulu et al., 2024). The primary binder phase in Portland cement, calcium silicate hydrate (C–S–H), is especially vulnerable. Acid exposure leads to progressive leaching of calcium hydroxide (portlandite), decalcification of the C–S–H gel, increased porosity, and ultimately, loss of structural integrity (Bogue, 1955; Herfort et al., 2010). These degradation pathways are not theoretical; laboratory studies have shown that Portland cement can lose more than 40% of its compressive strength after just 28 days of immersion in CO_2-saturated brine at 60 °C (Park et al., 2023; Wei et al., 2010). Field observations further confirm this risk long-term monitoring at the In Salah CO_2 storage project in Algeria revealed signs of wellbore degradation and pressure anomalies potentially linked to compromised cement integrity, prompting early suspension of injection (Salah, 2010). Thus, just like a sound drilling fluid design to ensure wellbore stability, it is also imperative to have a stable cementing system as well for CO_2 saturated conditions (Rasool and Ahmad, 2024; Rasool et al., 2022; Rasool et al., 2024a; Rasool et al., 2023a,b; Rasool et al., 2025; Rasool et al., 2021).

In response to these challenges, researchers and engineers have proposed a range of alternative cementing systems that claim enhanced acid resistance. These include modified Portland systems incorporating silica fume (Langan et al., 2002), fly ash (García-Lodeiro et al., 2013), or latex (Çolak, 2005) to densify the matrix and reduce permeability; non-Portland binders such as calcium aluminate cement (CAC) (Noor et al., 2023; Puri et al., 2010), magnesium phosphate cement (MPC) (Arora et al., 2019), and geopolymers (Bayuaji et al., 2017), which exhibit intrinsic resistance to acidic attack; and hybrid or resin-based systems designed for specialty applications. Nanomaterials, including nano-silica (Yu et al., 2014) and carbon nanotubes (Liu et al., 2022), have also been introduced to refine pore structures and delay acid ingress. Despite this growing toolbox, the cementing community lacks a clear comparative framework to evaluate these systems in terms of long-term durability, chemical performance, cost, and field scalability. Most existing studies examine isolated additives under differing test conditions, making it difficult to draw generalizable conclusions. Furthermore, there is little consensus on how to screen cement systems for CO_2 storage readiness. Standard API protocols, originally designed for hydrocarbon wells, are often inadequate in simulating the high acidity, supercritical CO_2, and complex brine compositions of storage reservoirs.

Given these pressing challenges and fragmented knowledge landscape, this review aims to critically assess the state-of-the-art cementing systems in context of for CO_2 storage wells. Rather than merely cataloguing available options, it interrogates the underlying mechanisms of resistance, scrutinizes the experimental methods used for validation, and proposes a multi-criteria screening framework helps in selection and validation of an optimal cementing cement for CO_2 storage wells. By integrating

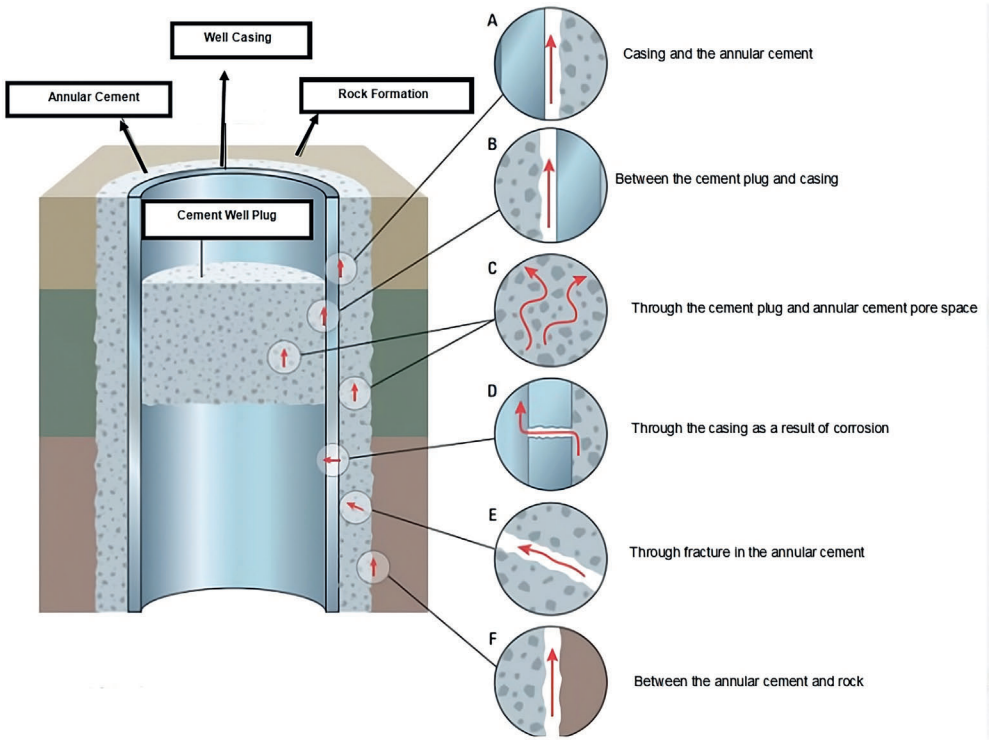

Fig. 1. Various possible scenarios of CO_2 leakage through cement (Ansarizadeh et al., 2015).

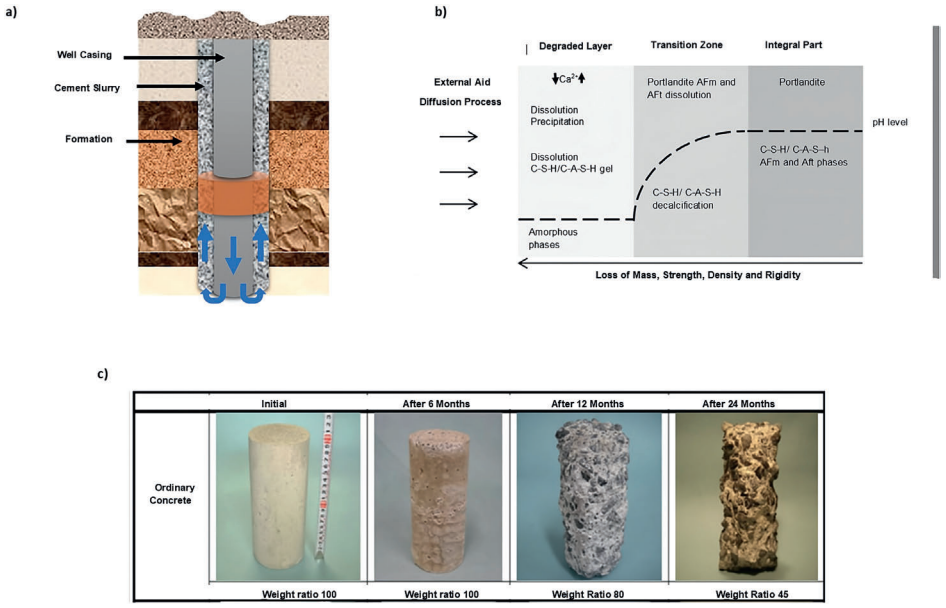

Fig. 2. Acid attack on cement sheath and vulnerability of cement degradation. a)Overview of cement sheath as a last defence for acid attack b)Acid diffusion process into cement sheath c)Example of cement degradation upon acid exposure (Japan Society of Civil Engineers, 2010; Irico et al., 2020).

insights from materials science, geochemistry, and field engineering, this work seeks to support the design of next-generation cement systems that are not only chemically robust but also field-viable and environmentally sustainable. In doing so, it aspires to bridge the gap between laboratory innovation and industrial implementation, an essential step if CCS is to be safely and reliably scaled in the coming decades. This review will fundamentally answer three research questions:

(1) How does CO_2 exposure degrade Portland cement in storage wells?

(2) Which acid-resistant cement systems best retain strength and resist carbonation under CO_2-brine conditions?,

(3) What are the best testing protocols and criteria for selecting durable cement systems for CO_2 storage?

2. API classes of Portland cement and mechanisms of degradation under CO_2 exposure

The American Petroleum Institute (API) classifies oilwell cements based on their performance under varying depths, pressures, and temperatures encountered during well construction. These standardized classes, designated as Classes A through H under API Specification 10A, are all variations of Portland cement, with different compositions and additives to tailor performance for specific downhole environments. For researchers and engineers developing acid-resistant formulations for CO_2 storage, understanding these cement classes is critical both as a baseline for comparison and as a matrix for modification. The specification of Class A-H has been reported from API 10A (Table 1) (American Petroleum Institute, 1995).

Class A and B cements are designed for shallow wells with low pressure and temperature. Class A is used when no special requirements are needed, while Class B is applicable in slightly more severe environments. Chemically, these cements contain a high amount of calcium silicates (C_3S and C_2S), which hydrate to form calcium-silicate-hydrate (C–S–H) and calcium hydroxide (CH). While C–S–H imparts strength, CH is highly soluble in carbonic acid and a primary point of failure in CO_2-exposed wells. Hence, these classes are rarely used or recommended for acid-rich environments. Class C cement is notable for its high early strength and elevated content of tricalcium aluminate (C_3A), which accelerates setting. While this property is beneficial in time-sensitive operations, it becomes a drawback in acidic conditions, as aluminates are vulnerable to sulphate and acid attack. Additionally, its high lime content (free CaO) makes it chemically unstable under prolonged CO_2 exposure. As such, Class C is generally unsuitable as-is for CO_2 storage applications unless modified heavily with pozzolanic or polymer additives (Jani and Imqam, 2021). Class D, E, and F cements are formulated for deeper wells, with higher pressure and temperature resistance (up to ~120–160 °C). These contain more belite (C_2S) than C_3S, making them slower to hydrate but more chemically stable in the long term. However, CH remains a major component of the hydration process. While they offer improved mechanical performance, these cements still require significant chemical modification to withstand acidic environments, such as the inclusion of silica fume or fly ash to consume free CH (Akbulut et al., 2024). Class G and H are the most used cements in oil and gas operations worldwide, especially for wells deeper than 3000 m. They are known for their predictable behaviour, low C_3A content, and adaptability to a range of additives. Their hydration produces fewer expansive phases, making them stable at high temperature and pressure. Despite this, their performance in CO_2-saturated brines remains inadequate without additive incorporation. In acid environments, Class G cement readily forms calcium carbonate ($CaCO_3$) when exposed to carbonic acid, leading to porosity increases and strength loss over time. For this reason, Class G is often used as the base matrix for testing acid-resistant additives such as nano-silica, CAC blends, graphene oxide, and latex (Alias et al., 2016; Kutchko et al., 2008, 2011; Nasvi et al., 2012; Samarakoon et al., 2021).

The fundamental limitation of all Portland-based API cement classes lies in their reliance on free CH for strength development, which also happens to be their Achilles' heel in acidic and CO_2-rich environments. Carbonic acid (H_2CO_3) reacts with CH to form soluble calcium bicarbonate [$Ca(HCO_3)_2$], which is easily leached out. Over time, this leaching leads to a weakened microstructure,

Table 1
Strength and Limitations of various API Portland cement classes for CO_2 storage wells.

Class	Typical Use Depth (m) (Est.)	Temp Range (°C) (Est.)	Key Composition	Strengths	Limitations in CO_2 Wells	Acid Resistance Suitability
A	0–600	Up to 60	High C_3S, moderate CH	Easy handling, general-purpose	High CH content, poor acid durability	Poor (requires major modification)
B	0–1200	Up to 85	High C_3S, some C_3A	Moderate-depth wells	Prone to carbonation and sulphate attack	Poor (prone to degradation)
C	0–1800	Up to 95	High early C_3S and C_3A	Fast strength development	Very reactive with acids and CO_2	Very Poor
D	1200–2400	85–120	Moderate C_3S and C_2S	Good thermal stability	Still produces CH; moderate acid resistance	Limited (needs SCMs or CAC blend)
E	1800–3000	120–140	High C_2S, low C_3A	High-pressure, high-temp wells	Slower hydration; moderate chemical durability	Moderate (requires pozzolans)
F	2400–3500	140–160	Higher belite (C_2S)	Suitable for ultra-deep wells	Hydrates slowly, CH still present	Moderate (needs chemical reinforcement)
G	600–3000+	Up to 120	Low C_3A, moderate C_3S	Highly versatile; standard reference cement	Reacts with $H_2CO_3 \rightarrow CaCO_3$, leading to strength loss	Moderate (excellent base for additives)
H	1800–4000	120–150	Low C_3A, high C_2S	Similar to G, better for deeper wells	Limited natural acid resistance; prone to CH leaching	Moderate (needs silica/fly ash etc.)

increased permeability, and eventual loss of zonal isolation (Lesti et al., 2013; Onan, 1984). This has spurred the exploration of alternative or hybrid systems such as Calcium Aluminate Cement (CAC), Magnesium Phosphate Cement (MPC), Geopolymers, and CAPC which either form no CH or generate phases inherently resistant to acid attack. Even within Portland-based systems, blending Class G or H with supplementary cementitious materials (SCMs) like silica fume, metakaolin, fly ash, or ground granulated blast furnace slag has proven effective in reducing the free CH content, enhancing C–S–H density, and improving long-term durability under CO_2-rich conditions (Barlet-Gouédard et al., 2009). Thus, the choice of cement class not only determines baseline performance but also dictates how and to what extent it must be modified to perform under the unique thermochemical stresses of CO_2 sequestration wells. Researchers aiming to design acid-resistant cements must start with this knowledge, as it informs additive selection, durability expectations, and scaling strategies for field deployment.

2.1. Why is the CO_2 storage environment corrosive?

In geological CO_2 storage operations, the injected CO_2 exists predominantly in its supercritical (sc-CO_2) state due to the high pressure and temperature conditions of deep subsurface formations. Supercritical CO_2 is achieved when the pressure exceeds 7.38 MPa and the temperature surpasses 31.1 °C conditions commonly found at depths greater than 800 m. In this supercritical state, CO_2 exhibits both gas-like diffusivity and liquid-like density, enabling it to efficiently permeate pore spaces and displace formation fluids. However, upon injection, CO_2 does not remain as a pure phase. It partially dissolves into formation brine, forming carbonic acid (H_2CO_3) (see equations (1)–(7)) (Carroll et al., 2016; Choi et al., 2013; Smith et al., 2010).

This results in a chemically aggressive environment known as sc–CO_2–saturated brine, characterized by low pH values (~3.0–3.5), high salinity, and the presence of corrosive anions such as Cl^- and SO_4^{2-}. The dual-phase presence of sc-CO_2 and acidified brine poses a significant threat to wellbore materials. Supercritical CO_2 can diffuse into microcracks and interfaces, while the brine phase initiates dissolution of cement hydrates, leaching of calcium, and progressive deterioration of the cement matrix. Therefore, understanding the phase behaviour of CO_2 and its interaction with both brine and cement is essential for the design and evaluation of acid-resistant cementing systems in storage wells. Once supercritical CO_2 ($scCO_2$) is injected into a deep saline formation or depleted hydrocarbon reservoir, it rapidly begins to interact with the resident brine and rock matrix. These interactions generate a suite of corrosive chemical species most notably carbonic acid (H_2CO_3) that initiate and sustain degradation pathways in cementitious materials.

Upon injection, CO_2 dissolves into formation water following Henry's Law (Enick and Klara, 1990):

$$CO_2\,(g) \rightleftharpoons CO_2\,(aq) \ldots \quad (1)$$

This is followed by hydration of aqueous CO_2 to form carbonic acid:

$$CO_2(aq) + H_2O \rightleftharpoons H_2CO_3 \ldots \quad (2)$$

Although H_2CO_3 is a weak acid, its presence lowers the pH of formation water significantly, often in the range of 3.0–4.5, depending on CO_2 partial pressure and brine buffering capacity. The carbonic acid then dissociates in two steps:

$$H_2CO_3 \rightleftharpoons H^+ + HCO_3^- (Ka_1 \approx 4.3 \times 10^{-7}) \ldots \quad (3a)$$

$$HCO_3^- \rightleftharpoons H^+ + CO_3^{2-} (Ka_2 \approx 5.6 \times 10^{-11}) \ldots \quad (3b)$$

The generation of H^+ ions from these dissociations directly contributes to the acidification of pore fluids. Under supercritical storage conditions (typically >7.38 MPa and >31.1 °C), CO_2 solubility in brine increases, thereby sustaining acidic conditions over time. For example, in the Sleipner field (North Sea), the injection zone lies at a depth of ~1 km with a temperature of ~37 °C and pressure near 10 MPa, while in deeper sites such as the Aquistore project (Canada), storage occurs at ~3.2 km depth, >110 °C, and pressures exceeding 30 MPa. Beyond carbonic acid, other in situ acids may also form depending on reservoir conditions and geochemical interactions. In formations with sulphide minerals, oxidation or bacterial sulphate reduction can lead to the formation of hydrogen sulphide (H_2S), which in aqueous form contributes additional acidity:

$$H_2S \rightleftharpoons HS^- + H^+ \ldots \quad (4)$$

In organic-rich or biodegraded reservoirs, the generation of low-molecular-weight organic acids (e.g., acetic, formic acids) can further reduce the pH and intensify the corrosive environment. These organic acids are known to accelerate cement matrix degradation by chelating calcium ions and destabilizing hydration products. These acidic species pose a direct threat to Portland cement systems. The initial attack begins with the dissolution of calcium hydroxide (portlandite), a highly alkaline phase that normally buffers pH:

$$Ca(OH)_2(s) + 2H^+ \rightarrow Ca^{2+} + 2H_2O \ldots \quad (5)$$

Following portlandite leaching, the calcium-silicate-hydrate (C–S–H) gel—the primary strength-contributing phase in hydrated cement—is progressively decalcified:

$$C\text{–}S\text{–}H(\text{Ca-rich}) + H^+ \rightarrow C\text{–}S\text{–}H(\text{Ca-poor}) + Ca^{2+} \ldots \quad (6)$$

This decalcification alters the gel structure, increases porosity, and eventually leads to disintegration of the solid matrix. Under CO_2 attack, another reaction pathway is carbonation, where dissolved CO_2 reacts with calcium ions to precipitate calcium carbonate:

$$Ca^{2+} + CO_3^{2-} \rightarrow CaCO_3(s) \ldots \quad (7)$$

While calcium carbonate precipitation may temporarily reduce permeability, it is not a permanent seal and may temporarily reduce permeability, it is not a permanent seal and may be prone to dissolution if pH decreases further or brine flow persists. Additionally, magnesium present in brines or rocks may react to form magnesium carbonates or brucite, further complicating the geochemistry.

2.2. Stepwise mechanism of Portland cement deterioration under CO_2-Induced acidic conditions

The subsequent sub-section outlines step-wise break down of Portland cement deterioration on CO_2-brine exposure, conditions in CO_2 storage wells as depicted in equations (8)–(13) (Agbasimalo and Radonjic, 2012; Barlet-Gouédard et al., 2007; Gaurina-Međimurec, 2010; Lesti et al., 2013; Zhang and Bachu, 2011).

Step 1: Formation of Carbonic Acid in the Subsurface.

When CO_2 is injected into a geological formation, it dissolves into the formation brine to form carbonic acid (H_2CO_3). This weak acid significantly lowers the pH of the pore fluid to values between 3 and 4, initiating the acidic attack on cementitious materials.

$$CO_2(g) + H_2O(l) \rightarrow H_2CO_3(aq) \ldots \quad (8)$$

This equilibrium exists under high CO_2 partial pressure (~10–25 MPa) and elevated temperatures (35–90 °C), which are typical of most deep CO_2 storage reservoirs.

Step 2: Dissolution of Portlandite (Calcium Hydroxide)

The first component to degrade is portlandite $Ca(OH)_2$ hydration product of tricalcium silicate (C_3S) and dicalcium silicate (C_2S). It is highly soluble in acidic environments and neutralizes H^+ ions rapidly.

$$Ca(OH)_2 + 2H^+ \rightarrow Ca^{2+} + 2H_2O \ldots \quad (9)$$

Alternatively, carbonic acid reacts directly:

$$Ca(OH)_2 + H_2CO_3 \rightarrow Ca_{2+} + CO_3^{2-} \ldots \quad (10)$$

This reaction depletes portlandite from the matrix and begins to destabilize the alkaline environment that protects cement integrity.

Step 3: Decalcification of C–S–H Gel.

After portlandite is exhausted, the next phase to degrade is the calcium silicate hydrate (C–S–H) gel, which is the main strength-contributing phase of Portland cement.

Hydrogen ions (H^+) or carbonic acid extract calcium ions from the C–S–H network, leading to depolymerization and structural collapse:

$$Ca_{1.5}SiO_{3.5}\cdot xH_2O + 2H^+ \rightarrow Ca^{2+} + SiO_2\cdot xH_2O + H_2O \ldots \quad (11)$$

The remaining silica gel is amorphous and poorly bound, increasing the porosity and weakening the matrix.

Step 4: Carbonation and Precipitation of Calcium Carbonate.

As free calcium ions accumulate in solution, they react with carbonate or bicarbonate ions to precipitate calcite ($CaCO_3$):

$$Ca^{2+} + HCO^{3-} \rightarrow CaCO_3(s) + H^+ \ldots \quad (12a)$$

$$\text{Or } Ca^{2+} + CO_3^{2-} \rightarrow CaCO_3(s) \ldots \quad (12b)$$

While the initial precipitation of calcite may reduce permeability by pore-filling, continued exposure to acidic conditions leads to re-dissolution of calcite and microcrack development due to volumetric changes.

Step 5: Expansion and Cracking due to Ettringite Formation (if SO_4^{2-} present)

If sulphate ions are present (from reservoir brine or bacterial H_2S oxidation), they react with aluminates to form ettringite, which causes internal expansion:

$$C_3A + 3CaSO_4 + 32H_2O \rightarrow \text{Ettringite} \ldots \quad (13)$$

Ettringite is expansive and can lead to crack propagation, debonding, and loss of well integrity, especially near casing–cement interfaces.

2.3. Stages of cement degradation upon CO_2 exposure

The deployment of conventional Portland cement systems in CO_2 storage wells has been inherited largely from oil and gas well construction practices. While such cement systems meet the immediate mechanical and operational requirements for well completion, they are often unfit for the long-term chemical and geomechanical challenges posed by CO_2-rich subsurface environments. As CO_2 reacts with formation brine and host rock, it creates aggressive acidic fluids that penetrate and degrade the cement sheath over time (see equations (14)–(16)). The resulting damage compromises zonal isolation and poses significant leakage risks. Understanding the specific failure mechanisms is essential for guiding the development of next-generation acid-resistant cement systems.

One of the earliest and most destructive chemical mechanisms of degradation in Portland cement systems is leaching, where soluble phases within the hardened matrix are dissolved and removed by acid attack. The first phase to be leached is usually calcium hydroxide (portlandite, $Ca(OH)_2$), which dissolves readily in acidic conditions (Carde and Francois, 1999):

$$Ca(OH)_2(s)+2H^+ \rightarrow Ca^{2+} \ldots \quad (14)$$

As the portlandite dissolves, the pH of the cement pore fluid declines from >12 to below 9, reducing the stability of the calcium-silicate-hydrate (C–S–H) gel. Progressive decalcification of C–S–H results in the gradual transformation of its structure into a weak, amorphous silica-rich gel:

$$C–S–HCa\text{-}rich+H^+ \rightarrow C–S–HCa\text{-}poor + Ca^{2+} \ldots. \quad (15)$$

This phase loses its binding capability, increasing porosity and permeability. In extreme cases, this mechanism transforms the cement into a chalk-like, friable structure incapable of resisting stress.

(1) Carbonation and Shrinkage

Simultaneously, carbonation reactions occur when dissolved CO_2 or bicarbonate ions interact with calcium ions from the cement matrix, precipitating calcium carbonate ($CaCO_3$) (Chen et al., 2006):

$$Ca^{2+} + CO_3^{2-} \rightarrow CaCO_3\,(s) \ldots \ldots \quad (16)$$

This reaction initially appears beneficial, as the $CaCO_3$ may form a protective carbonate rind near the exposed surface that temporarily reduces permeability. However, this layer is often non-uniform, brittle, and prone to cracking, especially under fluctuating injection pressures or thermal cycling. More importantly, the precipitation of $CaCO_3$ consumes free calcium from the matrix, further weakening C–S–H and promoting decalcification deeper into the cement structure. Moreover, carbonation can cause volumetric shrinkage, especially if it leads to the formation of vaterite or aragonite, which are less dense than portlandite or C–S–H. This shrinkage generates internal stresses and microcracks, weakening the matrix's ability to maintain zonal isolation.

(2) Crack Propagation, Micro-annulus, and Debonding

As porosity and shrinkage increase, microcracks begin to form, allowing deeper ingress of acidic fluids. Cyclic injection operations such as shut-in, falloff, and restart induce thermo-mechanical stresses that can widen these microcracks. Eventually, localized damage may extend to create a micro-annulus; a gap between the cement sheath and casing or formation. This micro-annulus acts as a high-permeability pathway for CO_2 migration, bypassing the sealing capacity of the cement (Ali et al., 2015).

Additionally, degradation at the cement–casing and cement–formation interfaces leads to debonding, which severely compromises mechanical anchoring and hydraulic isolation. SEM studies have shown that acid ingress concentrates at these interfaces due to stress concentration, imperfect mud removal, and elevated permeability. Once debonding initiates, the risk of radial and vertical leakage of CO_2 increases significantly, especially under high injection pressure.

(3) Strength Retrogression under Elevated Temperature

In many CO_2 storage sites, especially those at depths greater than 2 km, formation temperatures exceed 90–120 °C. Under these conditions, Portland cement experiences strength retrogression a process where long-term exposure to elevated temperatures leads to recrystallization of C–S–H into less cohesive crystalline phases like α-dicalcium silicate hydrate, tobermorite, or xonotlite. These phases are thermodynamically more stable but offer inferior mechanical integrity compared to the original amorphous gel(Reddy et al., 2016).

Strength retrogression is exacerbated by low water-to-cement ratios and poor pozzolanic reactivity. The result is a reduction in compressive strength, increased brittleness, and loss of elasticity features that make the cement sheath vulnerable to cracking and failure under subsurface stresses. This is particularly dangerous in cyclic injection scenarios where thermal expansion and contraction impose fluctuating loads. Fig. 3(a–c) illustrate the progressive degradation of Portland cement in CO_2-rich environments. The wellbore schematic and conceptual model highlight portlandite leaching, C–S–H decalcification, and strength loss mechanisms. Laboratory cores confirm this process, showing severe mass and structural deterioration after 24 months of exposure.

2.4. Effect of pressure, temperature and pH on cement degradation

The degradation of cement in CO_2 storage wells is not dictated by a single variable, but rather by the complex interplay of multiple physicochemical factors namely pH, temperature, pressure, and salinity each influencing the kinetics, thermodynamics, and extent of corrosive attack in different ways. The cumulative effect of these parameters shapes the severity of cement deterioration over time, and understanding their combined influence is crucial to developing and screening acid-resistant cement systems. One of the most dominant factors is pH, which governs the thermodynamic stability of cement hydration products. In Portland-based cements, the initial pore fluid pH ranges between 12.5 and 13.5 due to the dissolution of portlandite ($Ca(OH)_2$) and alkali ions. This high pH provides a protective environment, inhibiting the solubility of key hydration phases. However, when CO_2-rich brines infiltrate the cement matrix, carbonic acid (H_2CO_3) and other weak acids initiate a rapid drop in pH, often to values below 4 (Pearce et al., 2022; Takase et al., 2010; Udebhulu et al., 2024). This shift destabilizes the calcium-bearing phases, particularly portlandite, which dissolves readily according to eq. (17).

$$Ca(OH)_2\,(s)+2H^+ \rightarrow Ca^{2+} + 2H_2O \ldots \quad (17)$$

The loss of portlandite eliminates the cement's intrinsic buffering capacity, allowing protons to attack the calcium silicate hydrate (C–S–H) phase considered the backbone of the hardened matrix. As pH continues to drop, C–S–H undergoes decalcification, progressively transforming from a Ca/Si ratio >1.5 to <0.8, weakening its gel structure according to eq. (18).

$$C–S–HCa\text{-}rich+ H^+ \rightarrow C–S–HCa\text{-}poor + Ca^{2+} \ldots \quad (18)$$

Eventually, severely decalcified C–S–H transforms into amorphous silica gel, which is mechanically weak and poorly cohesive, leading to structural collapse. Moreover, the calcium ions released may react with available carbonate ions to form calcium carbonate polymorphs, such as calcite or aragonite as shown in eq. (19).

$$Ca^{2+} + CO_3^{2-} \rightarrow CaCO_3(s) \ldots \quad (19)$$

Although this carbonation reaction can reduce permeability temporarily by forming a dense carbonate layer, it is not a reliable long-term barrier. The carbonate crust is typically discontinuous, brittle, and prone to cracking under stress or pressure fluctuations, especially in cyclic injection operations.

Temperature plays a dual role while it accelerates the kinetics of acid-base reactions and diffusion processes, it also alters the stability of cement phases. In storage reservoirs, temperatures commonly range from 35 °C to over 120 °C, with deeper formations such as those at Aquistore or Tomakomai experiencing

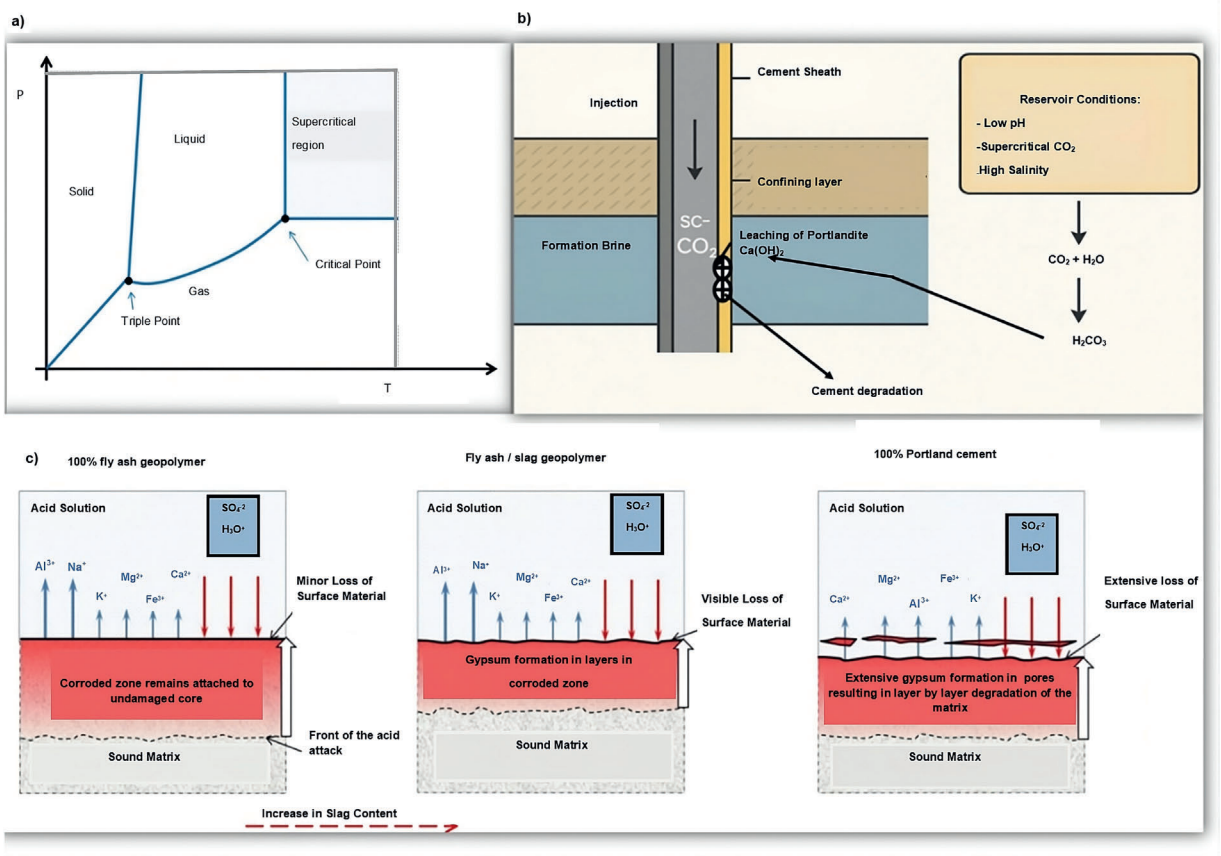

Fig. 3. Schematic illustration of supercritical CO_2 formation and its impact on cement degradation under reservoir conditions. (a) CO_2 phase diagram showing the transition to supercritical state above the critical point (31.1 °C, 73.8 bar). (b) Interaction of injected supercritical CO_2 (sc-CO_2) with the cement sheath and formation brine, leading to the generation of carbonic acid (H_2CO_3) and subsequent leaching of portlandite ($Ca(OH)_2$), initiating cement degradation. Reservoir conditions typically involve low pH (3.0–3.5), high salinity, and coexistence of sc-CO_2 and acidified brine. (c) Comparative acid resistance of different binders exposed to H_2SO_4 solution: 100% fly ash geopolymer exhibits only minor surface loss with corrosion confined to the outer zone; fly ash/slag geopolymers show gypsum formation in the corroded zone but maintain an intact sound matrix; while 100% Portland cement undergoes extensive gypsum precipitation in pores, causing progressive layer-by-layer degradation of the C–S–H and AFm matrix. Together, the panels illustrate the link between reservoir CO_2 conditions, acid-induced chemical degradation mechanisms, and the superior durability of alternative binder systems compared to conventional Portland cement (Aiken et al., 2018).

temperatures between 100 °C and 130 °C (Nath et al., 2024). At elevated temperatures, strength retrogression becomes a concern, especially for Class G Portland cement. This occurs due to the conversion of poorly crystalline C–S–H into more stable but weaker crystalline phases such as tobermorite or xonotlite, reducing the long-term mechanical performance. Furthermore, high temperature enhances the solubility of CO_2 in brines and increases the mobility of acidic species, exacerbating the depth and intensity of acid penetration into the cement sheath.

Pressure, particularly in supercritical CO_2 environments, introduces both mechanical and chemical implications. Pressures in deep injection wells can reach up to 20–35 MPa, sufficient to maintain CO_2 in a supercritical state. Supercritical CO_2 ($scCO_2$) has a lower viscosity but higher diffusivity compared to liquid CO_2, enabling it to infiltrate microcracks and interfacial voids more effectively. It can also co-exist as a free phase alongside CO_2-saturated brine, creating multiphase corrosive environments where cement is attacked from both liquid and gas interfaces. The partial pressure of CO_2 directly affects the amount of carbonic acid generated in the aqueous phase, with higher pCO_2 leading to lower pH and more aggressive chemical conditions.

Additionally, salinity of the formation brine modifies both the chemical activity and physical behaviour of the system. Brines in CO_2 storage targets are often highly saline, with total dissolved solids (TDS) exceeding 200,000 mg/L in some deep formations. The presence of sodium (Na^+), chloride (Cl^-), magnesium (Mg^{2+}), and sulphate (SO_4^{2-}) ions can interfere with cement hydration products through ionic substitution and competitive precipitation. For instance, Mg^{2+} can react with hydroxyl ions to form brucite ($Mg(OH)_2$), displacing calcium ions from C–S–H, while SO_4^{2-} may form expansive ettringite under certain conditions, contributing to cracking. High salinity can also lead to salt crystallization within cement pores during drying cycles, causing mechanical damage through expansion pressure (Al-Khdheeawi et al., 2018; Bachu, 2015; Bachu and Bennion, 2009; Gowthaman et al., 2016).

The combined effect of low pH, high temperature, elevated CO_2 pressure, and aggressive brine composition leads to accelerated degradation of traditional cement systems. This manifests not only as chemical dissolution but also as physical weakening, interfacial debonding, loss of zonal isolation, and increased permeability (see Table 2). In some field observations, such as in the Frio Brine test site (USA), CO_2 breakthrough was attributed in part to cement alteration zones where pH dropped below 4 and SEM images revealed clear signs of leached C–S–H and porosity increase near the casing interface.

Thus, any cementing system intended for use in CO_2 storage wells must be evaluated not just for compressive strength or thickening time, but for its resistance to acid dissolution,

carbonation, and mechanical degradation under reservoir-specific P–T–fluid regimes. Tailoring formulations to withstand these complex and variable conditions requires a fundamental understanding of subsurface chemistry, mineral stability, and reactive transport processes making geochemical robustness as important as engineering convenience in cement design for CCS.

2.5. Case studies of well integrity failures from CO_2 exposure

The In Salah CO_2 storage project in Algeria is one of the most cited cases of wellbore integrity compromise due to cement degradation. Injected at a depth of ~1.8 km with temperatures of ~95 °C and pressures of ~17 MPa, CO_2 at In Salah reacted with formation brine and migrated upward along a fault zone. Monitoring showed surface uplift and anomalous pressure behaviour, which were later linked to poor zonal isolation possibly resulting from cement sheath degradation and/or micro-annulus formation. Cement logging and well remediation efforts suggested interface debonding and permeability enhancement, consistent with chemical attack and mechanical failure mechanisms (Lanabi, 2024).

Another notable example is the Snøhvit project in the Barents Sea (Norway), where CO_2 (Oldenburg et al., 2011) was injected into a sandstone formation at depths of 2.6–2.8 km and temperatures near 90 °C. While the main storage formation showed good containment, some of the wells encountered operational issues, including injectivity decline and annular pressure buildup. Investigations indicated possible alteration of the cement and interfacial bonding due to prolonged exposure to acidic brines and thermal cycling.

Similar concerns have emerged from lab-based analog studies, such as the Frio pilot test (Texas, USA), where wellbore cement samples retrieved after CO_2 injection showed significant carbonation, Ca leaching, and reduced microhardness in the near-wellbore region. Microstructural analysis revealed porosity increase and mineralogical transformation, especially near the casing interface (Kharaka et al., 2009).

3. Types of acid-resistant cementing systems

Among the earliest strategies to improve the acid resistance of cement for CO_2 storage wells is the modification of conventional Portland cement using mineral and chemical additives. These so-called modified Portland systems retain the operational familiarity and basic chemistry of traditional Class G or H cement but introduce compositional and microstructural refinements to increase durability under aggressive acidic conditions. Strength percentages and carbonation depth of various cementing systems have been reported as Figs. 4–6. Primary mechanism and reaction conditions have been tabulated in Table 3. Furthermore, Table 4 provides a cross-category comparison that integrates performance, cost, and field applicability. This perspective highlights the trade-offs between durability and economic feasibility, showing that systems such as CAC and CAPC offer superior chemical resistance but face challenges of cost and scalability, whereas modified Portland systems remain cost-effective yet less durable under aggressive CO_2-brine exposure. Resin-based and nano-engineered systems exhibit excellent acid resistance but are constrained by cost or field readiness. Thus, Table 4 enables a decision-oriented view that complements the chemistry-based discussion and better reflects the practical considerations of CCS cement design.

3.1. Modified Portland systems

3.1.1. Latex modified

One of the most widely investigated strategies for improving the acid resistance of Portland cement systems is the incorporation of latex additives. Styrene-butadiene rubber (SBR) is among the most commonly used latexes, introduced to the cement slurry to improve flexibility, reduce permeability, and enhance bonding at the cement–casing and cement–formation interfaces. Latex particles form a dispersed polymeric film within the cement matrix, physically obstructing the transport of acidic fluids such as carbonic acid. This modification also enhances the hydrophobicity of the cement, thereby limiting water and CO_2 ingress. Studies have demonstrated substantial reductions in permeability and mass loss in latex-modified systems exposed to acidic brines. However, the long-term performance of these systems is highly dependent on downhole temperature. At temperatures exceeding 90 °C, latex can thermally degrade or coalesce, which compromises its function and may even result in phase separation or reduced matrix cohesion. Additionally, high latex content can delay setting times and reduce early compressive strength, which may be unacceptable in time-critical operations or high-pressure well environments (Hatungimana et al., 2020; John et al., 2023; Konduru, 2009; Yan et al., 2024; Yang et al., 2009).

Table 2
Degradation mechanism of various conventional PC cement system upon CO_2-brine/acid exposure.

Cement Type & Formulation	Exposure pH	Degradation Observations	Mechanism/Causes
Portland Class H neat $scCO_2$-saturated brine (0.5 M NaCl, 50 °C, 10 MPa) (Duguid et al., 2011; Duguid and Scherer, 2010)	~3–4	Carbonation depth ~2.1 mm after 30 d; $scCO_2$ achieved ~4.6 mm	Acid leaching of CH + decalcification of C–S–H; slower in brine vs $scCO_2$
Portland Class H neats $scCO_2$ (30 MPa, 50 °C) up to 1 year (Kutchko et al., 2008)	≈3 (carbonic acid)	Diffusion-controlled carbonation; limited CO_2 penetration when pre-cured under HPHT	Portlandite & C–S–H destabilization; $CaCO_3$ formation densifies near surface
Class H in reservoir brine embedded in sandstone/limestone (20–50 °C) (Duguid and Scherer, 2010)	3–7	In sandstone: 10 × permeability increase within 3 months; limestone: no degradation	Low-pH brine diffuses, leaches Ca, destabilizes C–S–H—dependence on host rock
Class G cement paste carbonic acid water (28 MPa and 80 °C) (Chavez Panduro et al., 2020)	6.08	Early-stage $CaCO_3$ fills pores + forms protective rind; long-term silica gel + shrinkage reduce strength	Initial pore blocking, but decalcification + amorphous silica precipitation degrades matrix
Class H (T = 30–80 °C) exposed to acid (pH 0–3.7) (Matteo and Scherer, 2012)	0–3.7	Corrosion rate increased sharply at pH < 3; especially high at 60–80 °C	H^+ aggressively attacks CH & C–S–H; temperature intensifies reaction rate
API Class G neat cured 40–120 °C; 10.5–14 MPa, $scCO_2$-brine (Binti Sauki and Irawan, 2010)	~3–4	At 90 °C & 20 MPa, fastest degradation observed; higher temperature increases carbonation front	Elevated T/P increase CO_2 solubility, diffusion, and H^+ attack depth

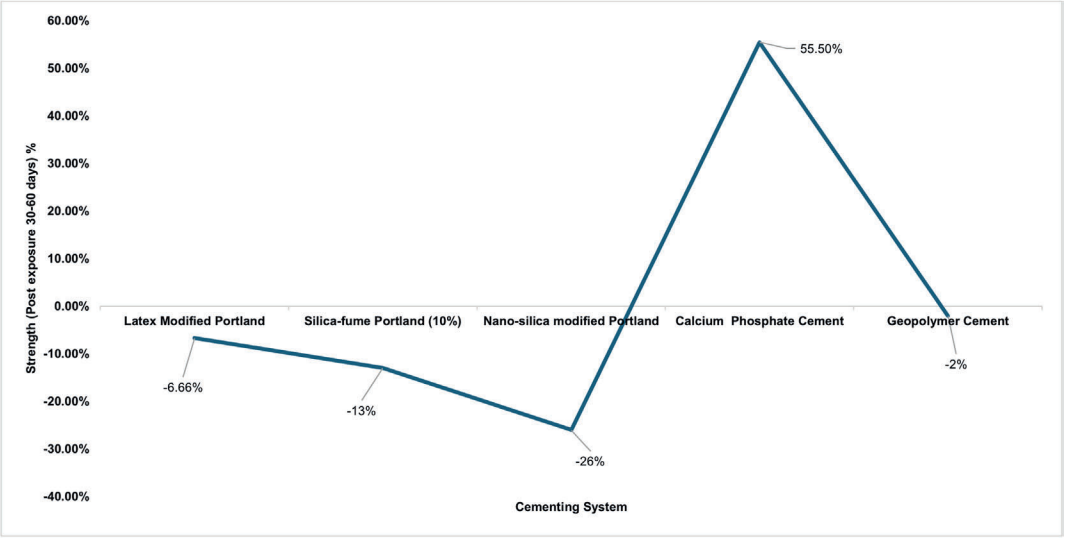

Fig. 4. Strength loss and gain; post CO_2-brine exposure for 30–60 days where CAC system shows gain in compressive strength even after exposure (comparing to control PC system) (Arshad et al., 2021; Beltrame et al., 2023; Sedić et al., 2024; Xin et al., 2020; Zhang et al., 2020).

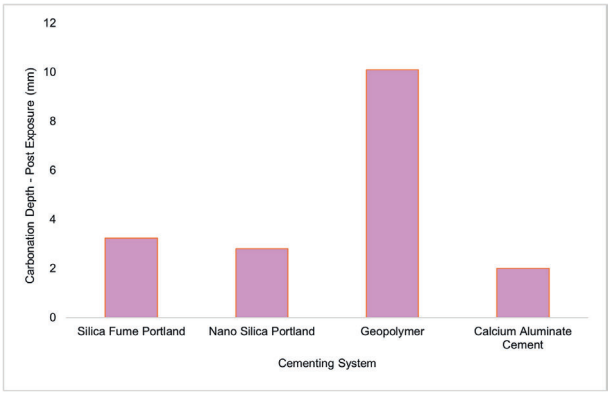

Fig. 5. Carbonation depth of various cementing systems post CO_2 brine exposure 30–60 days (Arshad et al., 2021; Beltrame et al., 2023; Sedić et al., 2024; Zhang et al., 2020).

3.1.2. Calcium aluminate blends

Blending Portland cement with calcium aluminate cement introduces alumina-rich phases that are inherently more resistant to acidic degradation. CAC hydrates into calcium aluminate hydrates such as CAH_{10} and C_2AH_8, which exhibit lower solubility in acidic environments compared to traditional C–S–H. These phases resist decalcification and carbonation more effectively and maintain their structural integrity even when exposed to CO_2-saturated brines. Additionally, CAC blends tend to form denser matrices with lower permeability, offering an extra barrier against acid ingress. One key advantage of CAC is its rapid setting and early strength development, which is beneficial for high-pressure or time-sensitive cementing operations. However, CAC systems are thermally sensitive. At elevated temperatures, the hydrates may undergo conversion to crystalline forms such as C_3AH_6, which have lower mechanical strength; a process known as strength retrogression. This conversion can be mitigated by blending CAC with pozzolans such as silica fume or fly ash to stabilize the hydration phases. Nevertheless, precise control of curing temperature, water-to-cement ratio, and admixture content is essential to avoid unintended performance losses. The higher cost and limited global availability of CAC also present practical barriers to its widespread adoption (Evju and Hansen, 2001; Gawlicki et al., 2010; Xu et al., 2017).

3.1.3. Pozzolanic additives

Pozzolanic additives such as silica fume, fly ash, and ground granulated blast-furnace slag (GGBFS) have been extensively used to densify the cement matrix and improve acid resistance through secondary hydration reactions. These materials react with free calcium hydroxide (portlandite) to form additional calcium-silicate-hydrate (C–S–H), thereby reducing the amount of highly reactive free lime available for acid attack. Silica fume, with its high surface area and fine particle size, is particularly effective in refining pore structures and increasing the continuity of the C–S–H phase. Fly ash, depending on its classification (Class F or Class C), contributes variable pozzolanic activity and can improve long-term chemical stability, while GGBFS introduces both latent hydraulic and pozzolanic reactivity. The reduced porosity and refined pore structure impede the penetration of aggressive acidic species. However, the pozzolanic reaction is relatively slow, and systems rich in these supplementary cementitious materials often suffer from delayed strength development and require longer curing times. Additionally, the effectiveness of pozzolans in improving acid resistance is highly sensitive to their composition, fineness, and curing temperature, making field performance somewhat variable unless rigorously controlled (Al-Chaar et al., 2011; Dembovska et al., 2017; Glasser et al., 1988).

3.1.4. Crosslinked polymer-latex matrices

A more recent innovation in the design of acid-resistant cement involves the incorporation of crosslinkable water-soluble polymers into the Portland cement matrix. These systems typically employ polyacrylamide, acrylic acid copolymers, or other functionalized polymers that undergo crosslinking upon hydration or exposure to elevated temperatures, forming a three-dimensional network within the hardened matrix. This polymeric mesh acts as both a physical and chemical barrier, impeding the transport of H^+ ions and stabilizing the microstructure against acid-induced leaching. In some cases, polymers are engineered with carboxylic or hydroxyl groups that interact with calcium ions or buffer localized pH changes. Cement formulations with crosslinked polymers have demonstrated impressive acid resistance under laboratory conditions simulating CO_2-rich environments, often

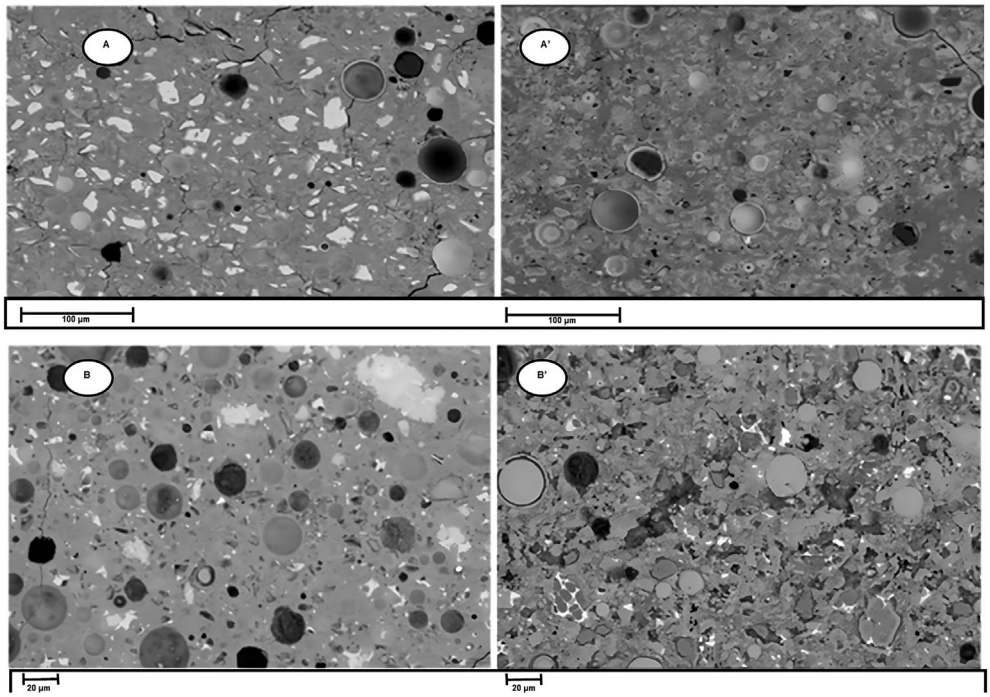

Fig. 6. SEM microstructural analysis showing pore evolution in cement matrices before and after CO_2 exposure. (A) Conventional Portland cement (PC) prior to CO_2 exposure, with relatively intact hydration phases and moderate pore distribution. (A′) Post-exposure PC reveals extensive pore coarsening, microcracking, and dissolution of calcium hydroxide and C–S–H phases, reflecting severe chemical degradation. (B) Calcium Aluminate Cement (CAC) before exposure, characterized by a denser matrix and finer pore structure. (B′) After CO_2 exposure, CAC retains a more compact microstructure with limited pore enlargement and reduced microcrack development, confirming its superior acid resistance compared to PC (Sedić et al., 2024). Scale has been manually drawn for more clarity.

retaining over 90% of compressive strength after prolonged exposure to carbonic acid at 80–100 °C. Despite these advantages, these systems are complex to formulate and relatively expensive. Their interaction with other cement additives, effect on slurry rheology, and placement behaviour under field conditions require careful optimization. Limited field trials also mean that their long-term performance and operational reliability under real reservoir conditions remain to be fully validated (Boodaghians, 1998; Fan et al., 2023; Guo et al., 2018; Wu et al., 2024).

Modified Portland systems, while diverse and widely studied, represent transitional solutions that attempt to retain the ease of deployment and familiarity of traditional oilfield cementing practices while improving chemical resilience. Their acid resistance is largely dependent on reducing permeability, minimizing free calcium content, and enhancing microstructural stability through secondary reactions or polymer reinforcement. However, none of these systems completely eliminate the underlying vulnerability of the C–S–H network to acid attack. Their field-scale efficacy remains contingent on proper formulation design, quality control, and adaptation to site-specific reservoir conditions. As such, while modified Portland systems may serve as practical short-to medium-term solutions, they do not provide a universally robust barrier for the century-long containment timescales demanded by CO_2 storage projects.

3.2. Non-Portland systems

3.2.1. Calcium aluminate cement (CAC)

Calcium aluminate cement has been extensively studied as a more chemically durable alternative to Portland cement, particularly in acidic environments. Unlike Portland systems that rely on calcium silicate hydrate (C–S–H) as the main binder phase, CAC hydrates to form calcium aluminate hydrates (CAH_{10}, C_2AH_8, and eventually C_3AH_6), which exhibit significantly greater resistance to acid attack. The aluminate phases are far less soluble in low-pH environments and are not prone to the same degree of decalcification as C–S–H. This intrinsic chemical stability allows CAC to maintain its structural integrity when exposed to CO_2-saturated brines, even at elevated temperatures. Additionally, CAC-based cements contain little to no free portlandite, thereby reducing the extent of early-stage leaching that typically initiates degradation in Portland cement. However, CAC systems are not without challenges. One major limitation is their susceptibility to strength retrogression due to the conversion of metastable hydrates into more stable but weaker crystalline forms, especially under high-temperature (>60 °C) curing. This phenomenon can be mitigated by controlling the water-to-cement ratio, adding pozzolanic materials, or using temperature-controlled curing protocols, but it remains a key design concern. CAC is also more expensive and less readily available than traditional cement, which may restrict its use in large-scale CCS operations. Nevertheless, CAC offers a significantly enhanced resistance profile for CO_2 storage applications, particularly where long-term exposure to acidic environments is expected (Damion and Chaunsali, 2022; Jahanbakhsh et al., 2021; Pyatina and Sugama, 2016; Sugama, 2006).

3.2.2. Calcium phosphate systems (calcium aluminate phosphate cement, CAPC)

Calcium phosphate-based cements, such as calcium aluminate phosphate cement (CAPC), represent a newer class of acid-resistant binders that combine the favourable properties of both aluminate and phosphate chemistry. These systems are typically formed by reacting calcium aluminate with acidic phosphate solutions, resulting in the formation of chemically stable phases like aluminum phosphate hydrates and hydroxyapatite ($Ca_5(PO_4)_3OH$). The key advantage of CAPC lies in its dual-phase stability:

Table 3
Acid resistance mechanism of various cement systems.

Cementing System	Primary Reaction or Component	Acid Resistance Mechanism	Acidic pH Resistance Range	Remarks	Limitations
Latex-modified Portland (Hatungimana et al., 2020)	Film-forming polymer; physical barrier	Hydrophobic film blocks H^+, CO_2 ingress	pH > 4.0	Thermally unstable above 90 °C	Thermal degradation, delayed set, limited long-term stability
Calcium Aluminate Blend (Evju and Hansen, 2001)	CAC hydration: CA + H_2O → CAH_{10}, C_2AH_8	Low Ca content; acid-stable aluminate hydrates	pH 3.5–5	Risk of strength retrogression >60 °C	High cost, conversion at elevated T, limited supply
Pozzolanic Blend (Al-Chaar et al., 2011; Dembovska et al., 2017; Glasser et al., 1988).	SiO_2 + $Ca(OH)_2$ + H_2O → C–S–H	Consumes portlandite; forms stable C–S–H	pH 4–6	Slow strength development	Slow reaction, dependent on curing, field variability
Crosslinked Polymer-Latex (Boodaghians, 1998; Fan et al., 2023)	Crosslinking polymers with Ca^{2+} and –COOH groups	3D polymer network resists H^+ and stabilizes microstructure	pH 3–5	Costly; complex mixing; thermal limits	High formulation sensitivity, cost, limited field validation
Calcium Aluminate Cement (CAC) Damion and Chaunsali (2022); Jahanbakhsh et al. (2021); Pyatina and Sugama (2016); Sugama (2006)	CA + H_2O → CAH_{10}, C_2AH_8 → C_3AH_6 (retrogression)	Minimal portlandite; acid-stable hydrates	pH 3–5 (if unconverted)	Durable if stabilized against conversion	Conversion risk without control, supply constraints
CAPC (Ca Aluminate Phosphate) (Liu et al., 2019; Plank, 2022; Živica and Bajza, 2001).	$CaAl_2O_4$ + H_3PO_4 → $Ca_5(PO_4)_3OH$ + $AlPO_4$ hydrates	Forms hydroxyapatite & $AlPO_4$ phases resistant to acid	pH 2.5–5	Stable under acidic brine	Needs precise synthesis pH; high cost; limited field data
Magnesium Phosphate Cement (Iyengar and Al-Tabbaa, 2007; Ribeiro et al., 2013, 2019; Yang et al., 2020).	MgO + $NH_4H_2PO_4$ + H_2O → $MgNH_4PO_4{\cdot}6H_2O$ (struvite)	No portlandite; acid-stable struvite binds matrix	pH < 3	Very rapid set and good early strength	Handling complexity; ammonia content; limited bulk application
Geopolymer Cement (Ridha et al., 2020; Ridha and Yerikania, 2015)	NaOH/Na_2SiO_3 + $Al_2O_3{\cdot}2SiO_2$ → N-A-S-H	Low Ca, forms acid-resistant aluminosilicate hydrates	pH 2.5–5	Green chemistry option	Requires high alkalinity; sensitive to curing and raw material variability
Epoxy Resin (Ajir et al., 2025)	Polyepoxide + hardener → crosslinked polymer matrix	Chemically inert, impermeable matrix	pH 1–4	High durability and adhesion	Expensive; not for bulk sections; curing sensitivity
Phenolic Resin (Anagnostopoulos et al., 2016; Baldissera et al., 2017; Ghassemi and Toufigh, 2020)	Phenol + formaldehyde + acid catalyst	Forms acid- and heat-resistant phenolic network	pH < 3	Strong chemical resistance	Brittle; limited data in CCS; handling complexity
Nano-silica (Ridha et al., 2018b)	SiO_2 (nano) + $Ca(OH)_2$ → C–S–H	Pozzolanic reaction consumes portlandite, densifies structure	pH 3–5	Improves durability and refines pores	Agglomeration, high water demand, cost
Nano-clay (Prakash et al., 2024).	Intercalation and Ca^{2+} buffering in silicate layers	Buffers H^+ ions and reinforces C–S–H structure	pH 3–5	Self-healing and impermeability potential	Agglomeration; affects rheology; dispersion issues
Graphene Oxide (GO) (Chuah et al., 2014; Pan et al., 2015; Zhao et al., 2020).	GO sheets + hydrates → cross-linking via –OH/–COOH groups	Physical barrier and crack bridging; acid inertness	pH 2.5–5	Good mechanical enhancement	High cost; complex mixing; scalability limitations

phosphate compounds are inherently resistant to acid dissolution, and the aluminum-rich matrix complements this resistance with low solubility and high chemical durability. CAPC systems also exhibit good early strength development and dense microstructures, making them attractive for downhole cementing applications. Laboratory tests have shown that CAPC can withstand immersion in carbonic acid (pH < 4) for extended periods without significant mass loss or structural degradation. Unlike Portland cement, which loses strength due to decalcification and carbonation, CAPC forms insoluble phosphate minerals that are stable across a wide pH range. The main limitations of CAPC include the need for precise pH control during synthesis, potential sensitivity to moisture, and relatively high raw material cost. Moreover, field experience with phosphate-based cements is limited, and their long-term performance in dynamic reservoir conditions remains to be comprehensively evaluated. Nevertheless, CAPC represents a highly promising candidate for wellbore sealing in CO_2 storage environments with extreme acidity and temperature (Liu et al., 2019; Plank, 2022; Živica and Bajza, 2001).

3.2.3. Magnesium phosphate cement (MPC)

Magnesium phosphate cement is another acid-resistant system that has gained attention for its rapid setting, high early strength, and exceptional durability in low-pH environments. MPC is formed by the reaction of dead-burned magnesia (MgO) with a soluble phosphate source typically ammonium dihydrogen

Table 4
Cross-category comparison of acid-resistant cementing systems in terms of performance, cost, and field applicability, highlighting trade-offs between durability under CO_2-brine exposure, economic feasibility, and operational readiness. Cost (Low-High) is relative based on current market prices.

Cement System	Performance (Acid Resistance & Durability)	Cost Level	Applicability in CO_2 Storage	Remarks
Modified Portland (SCMs, latex) (Hatungimana et al., 2020; John et al., 2023; Konduru, 2009; Yan et al., 2024; Yang et al., 2009)	Moderate; improved with pozzolans but still CH vulnerable	Low–Moderate	Field-proven in oil & gas, some CO_2 pilot sites	Transitional solution; affordable but not long-term robust
CAC (Calcium Aluminate Cement) (Damion and Chaunsali, 2022; Jahanbakhsh et al., 2021; Pyatina and Sugama, 2016; Sugama, 2006)	High; stable aluminate hydrates, resistant to CO_2 brine	High	Field-proven (blends in CO_2 wells)	Strong acid resistance; conversion risk at >60 °C
CAPC (Ca-Aluminate Phosphate) (Liu et al., 2019; Plank, 2022; Živica and Bajza, 2001)	Very High; forms stable phosphate/ hydroxyapatite phases	High	Lab-scale, emerging	Excellent durability, but expensive, limited field validation
MPC (Magnesium Phosphate Cement) (Iyengar and Al-Tabbaa, 2007; Ribeiro et al., 2013, 2019; Yang et al., 2020).	Very High; struvite formation, stable in pH < 3	High	Lab-scale only	Exceptional resistance; rapid set limits placement
Geopolymers (Kanesan et al., 2017; Ridha et al., 2017).	High; low-Ca gels resist carbonation/leaching	Moderate	Lab/pilot scale	Sustainable option; curing sensitivity
Resin-based (Epoxy/Phenolic) (Ajir et al., 2025; Anagnostopoulos et al., 2016; Baldissera et al., 2017; Ghassemi and Toufigh, 2020)	Excellent; inert, impermeable, withstands strong acids	Very High	Field-proven in remedial sealing, not bulk	Niche application; cost & handling challenges
Nano-engineered (SiO_2, GO, CNTs) (Camacho et al., 2014; Chen et al., 2011)	High; pore refinement, crack-bridging, added strength	Moderate–High	Mostly lab-scale	Promising, but dispersion/cost barriers
Hybrid Systems (e.g., Portland–CAC–nano blends) (Jahanbakhsh et al., 2021; Mahmoud, 2020; Sugama, 2006)	High; synergistic resistance, tailored microstructure	Moderate–High	Lab-scale, emerging pilot	Flexible design; complex QC needed

phosphate ($NH_4H_2PO_4$); in the presence of water. The primary hydration product, struvite ($MgNH_4PO_4{\cdot}6H_2O$), is chemically stable, exhibits excellent adhesion to metallic and non-metallic substrates, and resists both acid and sulphate attack. Because MPC does not produce calcium hydroxide as a byproduct, it avoids the common leaching and decalcification issues faced by Portland cement. Furthermore, MPC has been shown to maintain compressive strength in acidic solutions (pH < 2.5), even under thermal cycling. These properties make it well suited for CO_2 storage wells, especially in zones where rapid sealing or repair of micro-annuli is required. However, MPC's rapid setting time can pose placement challenges in deep wells, and the presence of ammonium may raise environmental or compatibility concerns in certain formations. The use of magnesium-based systems is also limited by cost and supply chain constraints, particularly in regions without easy access to magnesia or high-purity phosphate sources. While promising in laboratory settings, widespread adoption of MPC in CCS operations will require further validation under realistic reservoir conditions, including exposure to supercritical CO_2 and CO_2-saturated brines (Iyengar and Al-Tabbaa, 2007; Ribeiro et al., 2013, 2019; Yang et al., 2020).

3.2.4. Geopolymer cements

Geopolymers are synthetic aluminosilicate binders formed by activating source materials like metakaolin, fly ash, or slag with highly alkaline solutions such as sodium silicate and sodium hydroxide (Ridha et al., 2020; Ridha and Yerikania, 2015). Unlike traditional cements, geopolymers form amorphous or semi-crystalline sodium aluminosilicate hydrate (N-A-S-H) or calcium aluminosilicate hydrate (C-A-S-H) gels that are inherently low in calcium content. This absence of portlandite and other soluble calcium phases makes geopolymers highly resistant to acid attack and carbonation (Ridha et al., 2018a; Ridha and Yerikania, 2014). In acidic environments, geopolymers exhibit superior chemical stability, minimal leaching, and excellent resistance to strength loss, especially when cured properly (Kanesan et al., 2017; Ridha et al., 2017). Additionally, geopolymers have low permeability, high fire resistance, and reduced CO_2 footprints compared to Portland cement, aligning well with sustainability goals in CCS projects. However, their practical deployment is hindered by several factors. The need for highly alkaline activators raises safety and handling concerns during mixing and placement. Geopolymer formulations are also sensitive to curing conditions, particularly temperature and humidity, and may exhibit variable performance depending on the composition of raw materials (Ridha et al., 2017, 2018b). Furthermore, compatibility with casing materials and existing oilfield practices is not yet fully established, and there remains limited field-scale experience in CCS-specific applications. Despite these challenges, geopolymers hold strong potential as next-generation cementing materials, particularly for zonal isolation in storage formations characterized by long-term exposure to CO_2-saturated fluids (Haider, 2014; Nguyen et al., 2023; Peng, 2017; Zhao et al., 2024).

3.2.5. Resin-based cement systems (epoxy and phenolic resins)

Resin-based cements, including epoxy and phenolic systems, have been used for decades in remedial wellbore sealing, especially in geothermal and high-pressure environments. These systems cure into dense, crosslinked polymer matrices that are virtually impermeable and chemically inert in acidic and corrosive environments (Bett, 2017). Epoxy resins, in particular, are known for their excellent adhesion to steel and rock, high mechanical strength, and thermal stability up to 150 °C. Phenolic resins, although less common, offer superior chemical resistance in extreme acid conditions and high temperatures. Resin-based systems are particularly attractive for use in repair operations, casing leak mitigation, or as internal liners in CO_2 injection wells. Their resistance to H^+ diffusion, zero portlandite content, and high

elasticity make them robust candidates for harsh geochemical environments. However, their primary limitations lie in cost, placement difficulty in long or deep cement columns, and lack of bulk volume scalability for primary cementing. Resins also require precise mixing and curing controls, and their long-term mechanical compatibility with formation stresses remains a concern. Furthermore, the potential for thermal degradation or volumetric shrinkage during curing must be addressed, particularly in supercritical CO_2 environments. While unlikely to replace bulk cementing materials for full-length wellbores, resin systems remain valuable as targeted barriers in high-risk zones or for secondary sealing behind casing (Ajir et al., 2025; Anagnostopoulos et al., 2016; Baldissera et al., 2017; Ghassemi and Toufigh, 2020).

3.3. Nano-engineered systems

The incorporation of nanoparticles into cement systems represents a frontier approach in the development of acid-resistant barriers for CO_2 storage wells. By exploiting the unique physicochemical properties of nanomaterials such as high surface area, surface reactivity, and the ability to interact intimately with cement hydrates i.e., nano-engineered systems aim to enhance matrix densification, reduce permeability, and resist chemical degradation under low-pH and high-pressure conditions. These systems do not replace the primary cement chemistry but serve to augment performance by modifying the micro- and nano-scale structure of the hardened cement paste. Among the most studied nanoparticles in this context are nano-silica, nano-clay, graphene oxide, and carbon nanotubes, each offering distinct advantages in acid resistance and durability.

Nano-silica is one of the earliest and most extensively studied nanoparticles used in cement. With particle sizes typically ranging from 5 to 100 nm, nano-silica reacts rapidly with calcium hydroxide to form additional calcium-silicate-hydrate (C–S–H), leading to a denser microstructure with refined pore connectivity. This pozzolanic reaction consumes portlandite, which is otherwise highly susceptible to acid leaching, and replaces it with chemically more stable C–S–H. Additionally, nano-silica significantly reduces the connectivity of capillary pores, thereby hindering the ingress of CO_2 and acidic fluids. Experimental studies have shown that the inclusion of 1–2% nano-silica by weight of cement can result in substantial reductions in mass loss and porosity after immersion in CO_2-saturated brine. However, beyond optimal dosages, nano-silica may agglomerate, resulting in uneven distribution and localized weaknesses in the matrix. Its high reactivity also increases water demand and accelerates setting, which can complicate placement in field conditions (Batista et al., 2024; Singh and Islam, 2018).

Nano-clays, such as montmorillonite or halloysite, have also been investigated for their ability to intercalate into the C–S–H structure and enhance the resistance of cement to chemical attack. These particles offer layered silicate structures that can adsorb calcium ions and buffer proton diffusion, thereby reducing acid penetration. Additionally, their swelling properties upon hydration may help in sealing microcracks or interfacial voids, acting as a self-adaptive component in dynamic stress environments. When uniformly dispersed, nano-clays can significantly reduce permeability and enhance interfacial bonding with casing or formation rock. However, achieving homogeneous dispersion in cement slurries remains a significant challenge due to the strong tendency of nano-clays to form agglomerates. Moreover, their water-absorbing capacity can influence rheology and necessitate the use of superplasticizers or dispersing agents (Prakash et al., 2024).

Graphene oxide (GO), a two-dimensional carbon-based nanomaterial, introduces both mechanical and chemical benefits to cement systems. Its ultrathin planar structure, rich in oxygen-containing functional groups (e.g., –OH, –COOH), allows for strong chemical interactions with hydration products and promotes a continuous and chemically stable microstructure. GO has been shown to increase compressive strength, reduce water absorption, and improve resistance to carbonation. In acidic environments, GO's high chemical inertness and barrier-forming ability make it a potential additive for acid resistance. Furthermore, the presence of GO sheets can bridge microcracks, delaying crack propagation under stress and enhancing the fracture toughness of the cement. Nonetheless, graphene-based materials are currently expensive and difficult to scale, with reproducibility issues in large-batch formulations. Their impact on cement hydration kinetics and long-term durability under real CO_2 storage conditions remains an area of active research (Chuah et al., 2014; Pan et al., 2015; Zhao et al., 2020).

Carbon nanotubes (CNTs), both single-walled and multi-walled, offer remarkable mechanical reinforcement and may also serve to reduce ion diffusion through the cement matrix. Due to their high aspect ratio and strong bonding capability, CNTs have been proposed as nano-rebar to bridge microcracks and suppress permeability evolution under acid attack. Their inclusion in cement has shown improvements in tensile and flexural strength, as well as in durability metrics such as chloride and sulphate resistance. In the context of CO_2 storage wells, their ultra-low diffusivity could potentially serve as a secondary defence against acidic brine transport. However, challenges remain in ensuring uniform dispersion, preventing clumping, and maintaining consistency during mixing. Functionalization of CNT surfaces (e.g., carboxylation or hydroxylation) is often required to improve compatibility with the cement matrix, which adds complexity and cost (Camacho et al., 2014; Chen et al., 2011).

Despite their potential, nano-engineered cement systems are still in the early stages of deployment in CO_2 storage applications. While laboratory results are promising, field-scale data remain scarce. The behaviour of nanoparticles under long-term exposure to CO_2, elevated temperatures, and reservoir pressures is not fully understood, and there are concerns regarding nanoparticle leaching, environmental safety, and scaling feasibility. Moreover, the cost of high-purity nanomaterials, especially graphene and CNTs, can be prohibitive for bulk cementing applications. Nevertheless, with the advancement of scalable synthesis techniques and better dispersing agents, nano-engineered systems may offer a path toward creating low-permeability, chemically robust, and mechanically resilient cement barriers for next-generation CO_2 sequestration wells.

3.4. Hybrid systems

Hybrid cement systems are designed to leverage the strengths of multiple binder chemistries, creating a composite matrix that exhibits enhanced acid resistance, reduced permeability, and improved mechanical resilience under harsh CO_2 storage conditions. These systems typically integrate conventional Portland cement with components drawn from calcium aluminate, geopolymer, phosphate, or polymer-based formulations, aiming to overcome the individual limitations of each material. By carefully balancing mineralogical, chemical, and microstructural contributions, hybrid systems offer a pathway toward tailoring performance to specific reservoir environments while maintaining operational compatibility with existing cementing infrastructure (Jahanbakhsh et al., 2021; Mahmoud, 2020; Sugama, 2006).

One class of hybrid systems involves the partial substitution of Portland cement with both calcium aluminate cement and pozzolanic materials such as silica fume or metakaolin. The

Portland component contributes early compressive strength and workability, while the aluminate and pozzolanic additives introduce chemical durability and pore refinement. This combination helps to mitigate strength retrogression, reduce portlandite content, and promote the formation of acid-resistant hydrates like strätlingite and aluminosilicate gels. In CO_2-saturated brine environments, such ternary blends have demonstrated superior resistance to leaching and carbonation compared to any single-phase system. The key to success lies in the formulation: excessive aluminate content may trigger phase instability, while improper pozzolanic proportions can delay setting or compromise long-term strength (Pacewska et al., 2011; Vafaei and Allahverdi, 2016).

Another promising hybridization approach includes the use of geopolymer binders as secondary phases within a Portland-based matrix. These so-called "Portland–geopolymer hybrids" allow for gradual transition from traditional cement to low-calcium, aluminosilicate-rich systems (Tee and Mostofizadeh, 2021; Zhao and Sanjayan, 2011). The geopolymer component formed from activated fly ash or slag contributes to acid resistance and lowers the overall CO_2 footprint, while the Portland phase supports rheology control and early strength development. In hybrid systems cured under optimized conditions, the resulting matrix can contain both C–S–H and N-A-S-H phases, offering dual resistance mechanisms to carbonation and acid attack. These systems also benefit from a denser pore structure, reducing the rate of CO_2 diffusion and acid transport. However, their performance depends heavily on curing temperature, activator chemistry, and the interaction between the alkaline activator and Portland-derived phases. If not properly balanced, the two chemistries may compete, resulting in incomplete hydration or incompatibility at the microstructural interface.

Hybrid systems may also incorporate functional additives such as polymer dispersions, crosslinked hydrogels, or nano-reinforcements to improve crack resistance and durability under thermal cycling. For example, a blend of CAC–Portland–nano-silica–latex can deliver a dense, chemically stable, and flexible matrix capable of maintaining integrity even under acidic brine exposure and fluctuating temperatures (Xu et al., 2019). The polymer component enhances elasticity and seals microfractures, the nano-silica refines the pore network, while the dual cement phases provide complementary chemical resistance. Such systems are particularly attractive for high-risk zones in CO_2 wells, such as casing-shoe regions or fractured formations, where failure consequences are significant. Nonetheless, these complex multi-component systems require careful slurry design, compatibility testing, and quality control to ensure uniform mixing, predictable setting behaviour, and resistance to segregation under downhole conditions.

Despite their clear advantages, hybrid systems are still evolving and lack extensive field validation in CCS-specific projects. Most studies to date are laboratory-based, focusing on isolated aspects such as acid resistance or compressive strength, without fully evaluating long-term durability under real subsurface T–P–brine–CO_2 conditions. Their scalability and cost-effectiveness also remain under scrutiny, particularly in large-scale CO_2 injection projects where bulk volumes and logistical simplicity are critical. Nevertheless, hybrid cement systems represent a highly flexible and customizable approach to CO_2 well integrity and are likely to play a key role in future-proofing the cement sheath in next-generation carbon storage wells.

Figs. 4–6 collectively illustrate the comparative performance of different cement systems under CO_2-brine exposure. Strength retention and carbonation depth results (Figs. 4–6) clearly show the superior durability of CAC over conventional Portland systems, while SEM microstructural evidence (Fig. 6) confirms that CAC maintains a denser, less degraded matrix post-exposure. Together, these results validate the enhanced acid resistance of non-Portland binders for long-term CO_2 storage application.

Various favourable conditions for different acid/CO_2 resistant system have been tabulated in Table 5.

3.5. Key additives and their chemical functions

The effectiveness of acid-resistant cement systems in CO_2 storage wells hinges not only on the choice of base binder but also on the intelligent selection and optimization of chemical additives. These additives serve a wide range of functions from reducing permeability and enhancing acid resistance to modifying rheology and improving bonding with casing or formation (see Table 6). Their inclusion must be carefully calibrated to ensure compatibility with the cement matrix, durability under aggressive geochemical conditions, and stability at high pressures and temperatures.

Silica fume is one of the most widely used pozzolanic additives in acid-resistant formulations. Composed primarily of amorphous SiO_2 with particle sizes below 1 μm, silica fume reacts readily with calcium hydroxide (CH) liberated during Portland cement hydration to form secondary calcium-silicate-hydrate (C–S–H) gel. This pozzolanic reaction reduces the concentration of free lime highly vulnerable to acid attack and densifies the pore structure, thereby limiting CO_2 ingress. The resulting matrix exhibits enhanced chemical durability and reduced permeability. However, due to its high surface area, silica fume also increases water demand and may affect setting time if not properly balanced with superplasticizers.

Fly ash, particularly Class F fly ash, is another common additive that contributes both pozzolanic reactivity and long-term durability. It contains reactive aluminosilicates that react with CH and also promote the formation of acid-resistant gel phases such as strätlingite when blended with calcium aluminate cement. Its spherical particle morphology improves workability and reduces slurry viscosity, making it a favourable component in hybrid systems. In TSRC-type blends, fly ash has been shown to significantly enhance sulphate and acid resistance, particularly when activated with alkali silicates or phosphates.

Sodium hexametaphosphate (SHMP) functions as a dispersant and a chelating agent, particularly effective in reducing ionic interactions that could lead to premature flocculation in complex slurries. It can also sequester calcium ions in solution, reducing the formation of weak or soluble phases. In acidic environments, SHMP contributes to stabilizing the rheology of cement slurries and enhances acid resistance by minimizing the formation of leachable calcium phases. It is frequently used in combination with CAC, where it improves particle dispersion and inhibits early conversion of high-aluminate hydrates.

Latex additives, typically styrene-butadiene rubber (SBR), form flexible polymer films within the cement matrix that physically block the ingress of acidic fluids. Latex modifies the interfacial transition zone and improves bonding between cement and steel casing, reducing micro-annulus formation. In addition, its hydrophobic nature reduces water permeability, while its elasticity enhances resistance to thermal and mechanical stress-induced cracking. However, the thermal stability of latex must be considered, as polymer degradation above 90 °C can compromise performance in deep, high-temperature wells.

Nano-silica serves a dual function as both a pozzolanic material and a microstructure densifier. With a surface area up to 200 m^2/g, nano-silica reacts rapidly with CH to produce additional C–S–H gel while simultaneously filling capillary pores. This dramatically reduces permeability and improves early

Table 5
Favourable conditions for various Acid resistance cement systems.

Cement System	Effective pH Range	Suitable T Range (°C)	Suitable Pressure (MPa)	Strength Retention (Acid Exposure)	Current Status
Nano-Silica Modified Cement (Ridha et al., 2018b)	3–5	<100	≤20	High at 1–2 wt% dosage	Field-tested
TSRC (CAC + Fly Ash + Activator) (Hatungimana et al., 2020; John et al., 2023; Konduru, 2009; Yan et al., 2024; Yang et al., 2009).	0.5–2.5	Up to 90	Up to 20	Minimal loss at pH 0.5–2.5	Lab-proven, field data limited
CAPC/Hydroxyapatite-Based Cement (Liu et al., 2019; Plank, 2022; Živica and Bajza, 2001).	2–4	<100	≤20	Stable in CO_2-brine	Emerging/lab-scale
Magnesium Phosphate Cement (MPC) (Iyengar and Al-Tabbaa, 2007; Ribeiro et al., 2013, 2019; Yang et al., 2020).	<2.5	<120	≤25	Maintains 40–60 MPa	Lab-scale
Geopolymer Cement, (Ridha et al., 2017, 2018a)	2–5	<80 (typical)	≤25	Good strength retention; proven in lab settings	Pilot/lab only
Resin-Based Systems (Epoxy, Phenolic) (Ajir et al., 2025; Anagnostopoulos et al., 2016; Baldissera et al., 2017; Ghassemi and Toufigh, 2020)	<2	<150	≤30	Excellent resistance; no strength loss	Used in repairs/ remediation
Latex-Modified Portland Cement (Hatungimana et al., 2020)	4–6	<90	≤20	Moderate retention; performance drops above 90 °C	Field-proven
Silica Fume/Fly Ash/Slag Systems (Hatungimana et al., 2020; John et al., 2023; Konduru, 2009; Yan et al., 2024; Yang et al., 2009).	4–6	<120	≤25	Moderate to high (improves over time)	Widely adopted in well construction
Crosslinked Polymer-Latex Hybrids (Boodaghians, 1998; Fan et al., 2023; Guo et al., 2018; Wu et al., 2024)	3–5	60–100	≤20	High retention, but sensitive to formulation errors	Emerging (needs more field data)
Graphene Oxide–Modified Cement (Chuah et al., 2014; Pan et al., 2015; Zhao et al., 2020).	2–4	<120	≤20	High in lab studies; improves strength & durability	Experimental/lab-scale
Carbon Nanotube–Modified Cement (Camacho et al., 2014; Chen et al., 2011).	2–4	<120	≤20	High tensile/flexural strength; lab-scale only	Experimental/not field-validated
Portland–Geopolymer Hybrids (Haider, 2014; Nguyen et al., 2023; Peng, 2017; Zhao et al., 2024).	3–5	<100	≤25	Improved acid resistance with operational familiarity	Emerging/transitional system

compressive strength. In acid-rich environments, nano-silica-modified cements show reduced calcium leaching and enhanced retention of mechanical integrity. However, dispersion of nano-silica in water-based systems remains challenging, and agglomeration can result in localized weaknesses.

Graphene oxide (GO) and **carbon nanotubes (CNTs)** are emerging as high-performance additives for acid-resistant cements. GO provides two-dimensional nanosheets that can bridge microcracks and interact chemically with C–S–H through functional groups like –COOH and –OH. These interactions enhance mechanical strength and crack resistance while also introducing barriers to ion diffusion. CNTs, with their high tensile strength and nanoscale aspect ratio, act as nano-reinforcement and reduce microcrack propagation under stress. While both additives significantly improve mechanical durability, their high cost and dispersion difficulty limit large-scale application at present.

Alkaline activators, such as sodium silicate or sodium hydroxide, are essential components in geopolymer and hybrid systems. They dissolve amorphous aluminosilicates from fly ash or metakaolin and initiate polymerization reactions that result in the formation of N–A–S–H or C–A–S–H gels. These gels are inherently low in calcium and thus more stable in acidic environments. The choice and concentration of activator directly affect setting time, strength development, and chemical stability. Care must be taken to prevent alkali leaching and to ensure activator compatibility with other cement components.

Phosphate-based additives, such as ammonium dihydrogen phosphate ($NH_4H_2PO_4$) (or Potassium Dihydrogen Phosphate), are key to the formation of acid-resistant phases in calcium phosphate and magnesium phosphate cement systems. These additives react with magnesia or calcium aluminates to form chemically stable phases such as struvite or hydroxyapatite, both of which exhibit exceptional durability in acidic environments. Phosphates also contribute to rapid setting and early strength development, but their use requires careful pH control and may pose handling challenges.

Superplasticizers, particularly polycarboxylate ethers (PCEs), are indispensable in acid-resistant cement systems where pozzolanic or nanoparticulate additives are used. They enhance the flow properties of dense slurries, reduce water demand, and prevent particle agglomeration. In systems containing nano-silica, fly ash, or GO, the use of superplasticizers is often critical to achieving uniform dispersion and optimal microstructural performance.

Collectively, these additives represent the functional toolkit through which cement systems can be tailored to specific CO_2 storage well conditions. Their selection must consider chemical compatibility, thermal stability, dosage limitations, and the trade-offs between rheology, setting behaviour, and long-term durability. An intelligently formulated system often requires multiple additives working synergistically, with performance validated under simulated reservoir conditions to ensure effective zonal isolation and chemical resilience over decadal timescales.

Table 6
Mechanism and Limitations of key cementing system additives.

Additive	Function/Mechanism	Optimal Dosage (BWOC)	Performance/Outcome	Limitations/Risks
Silica Fume (Nochaiya et al., 2010)	Reacts with $Ca(OH)_2$ → extra C–S–H; densifies matrix and reduces permeability	5–15 %	↓ Porosity by ~30%; ↑ CO_2 corrosion resistance; improves strength and durability	High water demand; risk of delayed strength; needs superplasticizer
Fly Ash (Class F/C) (Dinesh et al., 2018; Papadakis, 1999)	Pozzolanic; forms secondary C–S–H and aluminosilicates; reduces CH; improves durability	10–30 %	Enhanced sulphate/acid resistance; good long-term strength	Variable reactivity; can slow early strength development
Nano-Silica (Shih et al., 2006)	Ultra-fine pozzolan; rapid CH consumption; fills nano porosity	1–3 %	↓ Permeability ~99%; ↓ porosity ~30%; strong early and long-term strength	Poor dispersion; agglomeration; high cost
Latex (SBR) (Hatungimana et al., 2020)	Polymer film blocks acid ingress; improves flexibility; reduces permeability	5–10 %	Improved CBL, reduced micro-annulus; better acid resistance vs neat cement	Thermal degradation >90 °C; slows setting; careful mixing required
Nano-Clay (Mont/Halloysite) (Amiri et al., 2022)	Layered silicate; ion buffering; microcrack swelling; reduces permeability	1–5 %	↓ Permeability, improved sealing under stress; lab—limited field data	Agglomeration; changes rheology; needs dispersants
Graphene Oxide (GO) (Chuah et al., 2014; Zhao et al., 2020)	2D barrier; chemical interaction with C–S–H; crack bridging; decreases diffusion	~0.2–0.5 %	↑ Elastic modulus +30%, ↑ compressive strength ~37%, ↓ permeability ~35%	High cost; dispersion challenges; scalability issues
Carbon Nanotubes (CNT) (Jayakumari et al., 2023; Reales and Toledo Filho, 2017)	Nano-reinforcement; bridges cracks; reduces diffusivity	~0.1–0.5 %	↑ Tensile & flexural strength; improved durability; lab-phase	Dispersion difficulty; high cost; risk of clumping
Polycarboxylate Superplasticizer (PCE) (Huang et al., 2016; Ma et al., 2023)	Reduces water demand; improves particle dispersion; enables low w/c dense slurries	0.2–1 %	Enables high-strength, low-porosity mixes with SCM/nanoparticles	Can alter setting profile; possible incompatibility
Sodium Hexametaphosphate (SHMP) (Cheng et al., 2020)	Chelates Ca^{2+}; disperses particles; helps stabilize slurry and buffer early acid	0.5–1 %	Improved acid/brine resistance; better rheology	Chelation may impact early set and strength
Ammonium Dihydrogen Phosphate (Defus et al., 2021)	Reacts with Ca/Mg to form stable phosphates (struvite, hydroxyapatite), rapid set	5–15 %	High early strength; excellent acid resistance in phosphate/MPC/CAPC systems	pH control essential; potential gas release; expensive
Nano-Alumina (Al_2O_3) (Jaishankar and Karthikeyan, 2017; Krishnaveni and Selvan, 2021)	Pozzolanic; boosts density; improves microstructure	0.5–2 %	Better durability; supports high-pozzolan systems	Alters setting; increases water demand
Hollow Glass Microspheres (Martín et al., 2023; Shahidan et al., 2017)	Density reduction; minimizes slurry density and mechanical mismatch	5–15 %	Low-density cement (<10 lb/gal); improves bonding and reduces fracture risk	Cost; may weaken compressive strength; careful mix required
Retarders (Lignosulphonates, Hydroxycarboxylic acids) (Fikeni et al., 2024; Yamamoto, 1972)	Control set; prevent flash setting; fine microstructure	0.1–1 %	Slower, more uniform hydration; better acid matrix continuity	Over-retardation risk; variable with temperature

4. Laboratory testing protocol for acid-resistant cement systems: a phase-based API tailored framework

Developing and validating cement formulations for CO_2 storage applications requires more than simple strength testing or pH exposure studies. To ensure a formulation's long-term durability under the harsh thermochemical conditions of CO_2 injection and storage, a structured, multi-phase testing protocol must be employed. This ensures that each system is evaluated not only for its mechanical performance under standard conditions but also for its chemical resistance, durability under thermal cycling, and integrity under acidified CO_2-rich brines. Drawing from American Petroleum Institute (API) specifications and recent advancements in durability testing, we propose a four-phase laboratory protocol, progressing from basic physical characterization to long-term acid resistance validation (see Fig. 5).

4.1. Phase I – baseline API cement characterization

The first phase focuses on evaluating the fundamental properties of the cement slurry and set cement using standardized procedures as outlined by API Specification 10B and 10A. This ensures that the formulation meets baseline performance for placement, safety, and operational use in the oilfield environment.

4.1.1. Slurry rheology – API RP 10B-2

The rheological evaluation of cement slurry is conducted according to API RP 10B-2 standards to ensure optimal pumpability,

flow stability, and placement behaviour parameters that are critical for the success of CO_2 storage well integrity. The test involves preparing the acid-resistant cement slurry using a high-speed blender, incorporating all relevant additives such as pozzolans, nano-silica, or latex according to the designed formulation. Slurry mixing typically follows the API procedure of blending at 4000 rpm for 35 s, followed by 15 s at 12,000 rpm. Once homogenized, the slurry is conditioned at ambient temperature (usually around 30 °C) for 60 min to simulate surface mixing and waiting-on-cement (WOC) intervals (Rodrigues et al., 2017).

Rheological measurements are then performed using a rotational viscometer (e.g., Fann 35 or equivalent) equipped with an R1–B1 rotor–bob assembly. The primary data points are taken at 100 rpm and 300 rpm to calculate plastic viscosity (PV) and yield point (YP), using the standard formulas: PV = 1.5 (300 rpm–100 rpm) and YP = 300 rpm - PV. These parameters help characterize the slurry's resistance to flow (PV) and its ability to suspend solids and prevent sedimentation (YP), which is especially important in horizontal or highly deviated injection wells commonly encountered in CO_2 sequestration projects (Al-Yami et al., 2017; Shahriar and Nehdi, 2012).

To capture the effect of downhole conditions, a secondary slurry batch is thermally conditioned at the expected bottomhole circulating temperature (BHCT), typically ranging between 60 °C and 100 °C depending on reservoir depth. This thermal conditioning can be performed in a pressurized consistometer before the viscometer readings, to simulate in-situ rheological behaviour during and after placement. Significant viscosity thinning or excessive gelation at BHCT can compromise the slurry's ability to provide effective zonal isolation or lead to undesirable pressure spikes during injection (Bannister, 1980; Hodne et al., 2000; Murtaza et al., 2016; Murtaza et al., 2016, 2016; Yang et al., 2024).

The results are interpreted critically. A plastic viscosity in the range of 30–80 cP is usually desirable lower values may risk turbulent flow, while higher values can induce excessive frictional losses. Yield points between 10 and 35 lb/100 ft^2 are generally acceptable, with values below 10 suggesting poor particle suspension and higher values indicating a tendency toward gelation and placement difficulties. The YP/PV ratio is also considered; values between 0.25 and 0.75 indicate a stable flow regime. Ultimately, this rheological profile is used to optimize both the cement slurry formulation and the pumping schedule to suit the specific challenges posed by the target CO_2 storage formation.

4.1.2. Thickening time – API RP 10B-2

Thickening time testing, as prescribed by API RP 10B-2, is a critical parameter in designing cement systems for CO_2 storage wells. This test is performed using a pressurized consistometer, which simulates the downhole thermal and pressure conditions typically encountered in CO_2 injection zones commonly ranging from 60 to 90 °C and 10–25 MPa. The objective is to determine the duration during which the slurry remains in a fluid state suitable for pumping, displacement, and placement in the wellbore before setting begins. The slurry is loaded into the consistometer and stirred continuously while being subjected to the programmed temperature-pressure ramp based on the reservoir profile. The test is considered complete when the slurry reaches 70 Bearden Consistency Units (BCU), a threshold which indicates the onset of thickening and loss of pumpability (Al-Yami et al., 2017; Chen et al., 2021).

For CO_2 wells, a well-designed slurry should exhibit a thickening time of at least 3–4 h under downhole conditions, providing ample operational margin for placement, especially in long or deviated wells (Al-Yami et al., 2010; Bett, 2017; Krueger, 1986). Equally important is a sharp viscosity transition, indicating rapid gelation after the desired placement window (Lota et al., 2013; Salam et al., 2013), this minimizes the risk of free water separation or incomplete zonal isolation. Slurries with prolonged transition zones or unpredictable thickening behaviour can lead to channelling, micro-annulus formation, or fallback. Additionally, thermal stability of the additives used (e.g., retarders, dispersants, or pozzolanic fillers) must be validated during this test, as excessive retardation or instability at high temperatures can severely compromise set integrity. For systems incorporating acid-resistant binders like CAPC, geopolymers, or CAC, customized temperature ramps may be needed to reflect slower kinetics or non-Portland setting behaviour.

4.1.3. Free fluid test – API RP 10B-2

The free fluid test, conducted according to API RP 10B-2, is designed to assess the slurry's stability under static conditions by measuring the amount of free water that separates from the cement phase. In the context of CO_2 storage wells, where long static periods may occur during placement or prior to setting, ensuring minimal water separation is essential to prevent formation of weak zones, density gradients, or micro-annuli. The test is typically performed by placing a known volume of freshly mixed slurry into a vertical, graduated, cylindrical container and allowing it to rest undisturbed at either ambient or simulated downhole temperature. After 2 h, the volume of supernatant liquid is recorded and expressed as a percentage of the total slurry volume. Free fluid test should be at vertical and 45°. For Class G cement, an acceptable threshold is typically $\leq$1.5% free fluid, although tighter limits ($\leq$1.0%) are often targeted for critical wells (Karakaya and Kök, 2013; Mahmoud, 2024a, 2024b).

In acid-resistant cement systems especially those incorporating pozzolanic additives, latex polymers, or nanoparticle suspensions the interaction of additives with water can either exacerbate or mitigate fluid separation. For example, silica fume and nano-silica increase slurry stability by forming a denser gel network, while excessive dispersants or unbalanced retarders may promote water release. A high free fluid value not only indicates poor formulation design but also raises the risk of CO_2 channelling during early gas breakthrough, particularly if the upper annular regions are inadequately filled. In CO_2 wells, maintaining a low free fluid content is vital to ensure uniform hydration, reduce shrinkage-induced cracking, and enhance zonal isolation under acidic and thermobaric stress conditions (Al-Yami, 2015b; Blount et al., 1991; Cestari et al., 2012; Gaurina-Međimurec et al., 2021).

4.1.4. Sedimentation stability – API RP 10B-4

The sedimentation stability test, outlined in API RP 10B-4, is essential for evaluating the vertical homogeneity of a cement slurry after it has been allowed to set under static conditions (Doan et al., 2017; Gruber and Plank, 2020). This test simulates real downhole scenarios, particularly in CO_2 storage wells where extended static periods before setting are common. A cement slurry with poor sedimentation stability may exhibit phase separation, where denser particles settle and create a gradient in mechanical strength and permeability along the column(Costa et al., 2021; Kremieniewski et al., 2017). The test is conducted by preparing a sample of the slurry, placing it in a vertically oriented mold or column, and curing it under simulated downhole temperature and pressure. After curing, the column is sectioned typically into top, middle, and bottom segments and each section is weighed and analysed to determine density variations. A density differential greater than 0.2 g/cm^3 between the top and bottom segments is considered unacceptable and suggests severe instability or inadequate suspension capacity (Gandelman et al., 2004; Wang et al., 2025).

This parameter becomes particularly critical in CO_2 wells where acid-resistant systems such as CAC, CAPC, or geopolymer formulations are used, often in combination with microfine additives or supplementary materials (Silva et al., 2012; Zhang et al., 2024). These slurries may have altered settling behaviour due to differences in particle morphology, surface charge, or hydration kinetics. For instance, heavy pozzolanic blends or nano-additives may increase viscosity yet still suffer from density segregation if not properly dispersed. Poor sedimentation stability not only compromises compressive strength distribution but also increases the risk of preferential CO_2 migration through weaker, underdense zones (Liu et al., 2018). Therefore, achieving sedimentation stability within the allowable range is a strong indicator of overall slurry performance and robustness under static column conditions in deep, long-life CO_2 injection wells.

4.1.5. Compressive strength development – API RP 10B-2

Compressive strength development, as outlined in API RP 10B-2, is one of the most fundamental performance indicators for any cement system, particularly those intended for long-term CO_2 storage applications. The test involves preparing either cubic or cylindrical cement specimens and curing them under reservoir-representative temperature and pressure conditions typically between 60 and 90 °C and up to 25 MPa, depending on the storage depth. The samples are demoulded and subjected to uniaxial compression at defined time intervals (commonly 8, 24, 48, and 72 h) using a calibrated compressive load frame. The strength values obtained reflect the hydration kinetics, degree of gelation, and phase development within the cement matrix. A target strength of at least 3.5 MPa (500 psi) is typically required for surface casing applications, while a minimum of 6.9 MPa (1000 psi) is recommended for intermediate and deep injection zones (Ashraf et al., 2024; Hussain, 2021; Mueller, 2012; Yang et al., 2024).

In the context of CO_2-resistant cement systems such as CAC, CAPC, geopolymers, and pozzolan-augmented Portland cement the strength development curve also provides insight into long-term chemical stability. Unlike traditional OPC systems, which develop strength rapidly but may degrade under acidic exposure, alternative binders may show slower early strength gain but superior resistance to acid-induced decalcification and microstructural weakening (Joel and Ademiluyi, 2011; Lesti et al., 2013; Wang et al., 2022). It is essential to monitor not only peak compressive strength but also its retention post-exposure to CO_2-saturated brines, which can simulate field degradation scenarios. Moreover, the correlation between early strength and thickening time ensures that the slurry reaches operational maturity within safe handling windows, without compromising structural integrity. Therefore, compressive strength development is both a mechanical and chemical performance marker for acid-resistant cementing systems tailored to CO_2 storage wells (Falode et al., 2013; Mozaffari et al., 2022).

4.2. Phase II – durability & thermal stability evaluation

Phase II assesses how the cement performs under thermal and hydrothermal conditions expected in CO_2 storage formations. This step ensures the cement can resist strength retrogression and maintain structural integrity over time at elevated T–P.

4.2.1. Autoclave curing (thermal aging) – API RP 10B-5

Autoclave curing, governed by API RP 10B-5, simulates prolonged thermal and pressure exposure to evaluate the long-term durability of cement systems under downhole conditions relevant to CO_2 storage wells. In this method, prepared cylindrical or cubic cement specimens are cured in an autoclave at temperatures typically ranging from 60 °C to 120 °C and pressures up to 25 MPa, closely replicating subsurface conditions in deep saline aquifers or depleted reservoirs. The curing durations commonly span 3, 7, and 28 days to assess the progressive development of hydration products, microstructural stability, and chemical robustness over time. These conditions are particularly relevant for acid-resistant systems that undergo phase evolution beyond the initial 72 h such as the transformation of metastable hydrates into thermally stable phases like stratlingite in CAC, or apatite in CAPC (Kang et al., 2023; Yang et al., 2013; Yu et al., 2023).

After curing, the samples undergo a series of evaluations. Physical integrity is first assessed through visual inspection, noting any signs of cracking, discoloration, or efflorescence, which may indicate chemical instability or thermal shrinkage. The samples are then retested for compressive strength to determine strength retention or degradation under aging. Additionally, ultrasonic pulse velocity (UPV) measurements are performed to assess internal homogeneity and detect microcracking or pore coalescence, which may not be evident visually. A stable or increasing UPV reading indicates good microstructural integrity, while a drop may signal microdamage or degradation. In CO_2 storage cement qualification workflows, autoclave curing serves as a critical aging test to predict long-term performance under sustained thermobaric exposure, helping differentiate systems that merely meet early strength targets from those that can maintain integrity over decades of CO_2 exposure.

4.2.2. Ultrasonic cement analyzer (UCA) – API RP 10B-5

The Ultrasonic Cement Analyzer (UCA), as specified in API RP 10B-5, is a non-destructive method used to monitor the real-time development of compressive strength in cement slurries under high-pressure, high-temperature (HPHT) conditions. This technique is particularly valuable for evaluating acid-resistant cement systems used in CO_2 storage wells, where early strength development under thermobaric stress is a critical performance indicator. In UCA testing, the cement slurry is placed in a pressurized test cell maintained at the target bottomhole circulating temperature (typically 60–120 °C) and pressure (up to 25 MPa). As the slurry begins to hydrate and set, the instrument transmits ultrasonic pulses through the sample. The transit time of these pulses is continuously recorded and correlated with compressive strength via a calibrated empirical relationship (Arbad et al., 2021; Chotard et al., 2001; Panchmatia et al., 2019).

This method is especially advantageous for acid-resistant binders that exhibit atypical or nonlinear setting behaviour such as magnesium phosphate cements (MPC), geopolymers, and calcium aluminate phosphate systems where conventional destructive strength tests may not capture early gelation or stiffness transitions accurately. UCA provides a complete strength–time curve, allowing researchers to observe induction periods, acceleration phases, and final set points in a continuous and automated manner. Such detailed profiles are essential for optimizing additive loadings, retarder concentrations, and accelerator dosages to balance pumpability with early resistance to CO_2 ingress (Nascimento et al., 2022; Wagner et al., 2021). Additionally, UCA helps identify undesirable setting anomalies (e.g., flash setting or prolonged dormancy) that may compromise operational performance. In CO_2 storage cement design workflows, UCA thus serves as both a screening and validation tool for early-age behaviour under representative subsurface conditions.

4.2.3. Thermogravimetric Analysis (TGA) and Differential Scanning Calorimetry (DSC)

Thermogravimetric Analysis (TGA) and Differential Scanning Calorimetry (DSC) are powerful thermal characterization

techniques used to evaluate the phase composition, thermal stability, and hydration product evolution in cement systems particularly those designed for CO_2 storage applications. These techniques are especially valuable for analysing acid-resistant formulations such as calcium aluminate cement (CAC), calcium aluminate phosphate cement (CAPC), and other non-Portland binders where traditional XRD may not effectively quantify amorphous or transient hydration phases.

In TGA, the cement sample is heated in a controlled atmosphere (typically nitrogen or air) from ambient temperature to around 1000 °C at a fixed ramp rate (e.g., 10 °C/min), and the corresponding weight loss is continuously recorded. Distinct weight loss intervals correspond to the decomposition of specific hydration products. For example, the decomposition of calcium hydroxide (CH) typically occurs between 400 and 500 °C, allowing for quantitative estimation of portlandite content, while dehydration of C–S–H gels generally occurs below 200 °C. In CAC systems, TGA is particularly useful in detecting the conversion of metastable hydrates like CAH_{10} and C_2AH_8 into the more stable but denser and less volumetrically supportive C_3AH_6 phase, which occurs between 200 and 350 °C and is critical for long-term performance prediction (Huo et al., 2021; Mohammed et al., 2020; Wang et al., 2024).

Complementary to TGA, DSC provides thermal event profiles by detecting endothermic or exothermic reactions during heating. It allows identification of phase transitions (e.g., crystallization or dehydration) and their associated enthalpy changes, offering insight into the energetic stability of the hydration products. The combination of TGA–DSC enables the assessment of phase integrity under elevated temperatures, aiding in the optimization of formulations for thermal durability and resistance to acid-induced decalcification. For CO_2 storage well cementing, this dual technique is indispensable for verifying whether the hydration system maintains chemically stable, low-porosity phases over time, particularly under the cyclic heating and acidic exposure conditions typical of injection and shut-in cycles (Sanderson et al., 2017; Vieira et al., 2004).

4.3. Phase III – acid resistance testing & chemical durability

In this phase, the cement is tested for resistance to CO_2-saturated brine and synthetic acids to simulate long-term downhole exposure. This phase moves beyond mechanical strength to chemical integrity.

4.3.1. Immersion testing (carbonic acid exposure)

Immersion testing under carbonic acid exposure or brine-CO_2 exposure is a critical durability assessment method for evaluating the long-term performance of acid-resistant cement systems in CO_2 storage well environments. In this test, cured cement core samples are submerged in CO_2-saturated synthetic brine typically comprising 1–1.5 M NaCl to replicate the geochemical conditions of deep saline aquifers. The brine is equilibrated with CO_2 to achieve a pH of approximately 3.5, which simulates the carbonic acid generated in situ when injected CO_2 dissolves in formation water. Samples are then exposed at reservoir-representative temperatures and pressures (commonly 60–90 °C and up to 25 MPa) using autoclaves or high-pressure reactors for defined durations of 7, 14, and 28 days (Bertron, 2012; Bertron et al., 2005, 2007; Teodoriu and Bello, 2020).

Following exposure, the samples are evaluated for compressive strength retention using standard uniaxial testing protocols, and mass loss is recorded to quantify material degradation. A significant reduction in compressive strength or increase in mass loss is indicative of leaching, decalcification, or phase decomposition. Additionally, the pH of the brine is monitored before and after immersion to assess the buffering capacity of the cement system and track acid neutralization kinetics. For systems like calcium aluminate cement (CAC), calcium aluminate phosphate cement (CAPC), or geopolymers, minimal pH drop and strength loss typically reflect the formation of stable hydrates such as strätlingite, hydroxyapatite, or N-A-S-H gels. Conversely, conventional Portland cement tends to show rapid strength decay and increased porosity due to the dissolution of calcium hydroxide and destabilization of C–S–H phases. Immersion testing therefore provides a direct simulation of field-relevant chemical exposure and serves as a benchmark for acid durability in CO_2 sequestration cement formulations (Teodoriu and Bello, 2020; Xie et al., 2004).

4.3.2. Mass loss analysis

Mass loss analysis, adapted from ASTM C267, is a quantitative method used to evaluate the chemical durability of cement systems when exposed to acidic environments particularly relevant for CO_2 storage wells where prolonged contact with carbonic acid can lead to matrix dissolution and structural weakening. In this procedure, cement specimens (typically cylindrical or prismatic) are accurately weighed before immersion and then subjected to controlled exposure in CO_2-saturated brine (pH ~3.5) at reservoir-simulated conditions typically 80–100 °C and pressures up to 10 MPa for durations ranging from 7 to 28 days (Consoli et al., 2018; Naik et al., 2001).

After the exposure period, samples are gently rinsed, dried to constant weight, and reweighed to determine the percentage mass loss, which reflects the extent of material degradation, particularly from leaching of calcium phases and disintegration of the cement matrix. For a cement system to be considered acid-resistant, the mass loss after 28 days should generally remain below 5%. Portland cement systems often exceed this threshold due to the high solubility of calcium hydroxide and destabilized C–S–H under acidic attack. In contrast, advanced systems such as CAC, CAPC, and geopolymers exhibit significantly lower mass loss due to the formation of chemically stable hydrates like strätlingite, hydroxyapatite, and aluminosilicate gels that are less prone to acid dissolution. Mass loss analysis, when combined with compressive strength and pH monitoring, offers a comprehensive understanding of acid-induced deterioration and is vital for screening and validating cement formulations intended for long-term CO_2 sequestration environments (Lv et al., 2022).

4.3.3. Scanning Electron Microscopy (SEM) and EDS mapping

Scanning Electron Microscopy (SEM) coupled with Energy Dispersive X-ray Spectroscopy (EDS) mapping is a vital microanalytical technique for assessing the degradation mechanisms of cement systems exposed to CO_2-rich environments. In the context of CO_2 storage wells, where acid–cement interactions occur at both chemical and microstructural levels, SEM enables high-resolution imaging of surface and cross-sectional morphologies to detect features such as microcracks, porosity changes, etching, and phase disintegration. After immersion in CO_2-saturated brine, cement samples are sectioned, resin-impregnated (if needed), polished, and gold- or carbon-coated for SEM analysis. High-magnification imaging allows identification of deteriorated interfaces, weakened gel phases, and the progression of carbonation fronts (Bin Abed, 2024; Chavez Panduro et al., 2017; Jahanbakhsh et al., 2021).

The integration of EDS provides spatially resolved elemental maps, enabling semi-quantitative analysis of leached species (such as Ca, Si, Al, P) and identification of reaction zones. One of the most crucial applications in acid-resistant cement systems is detecting carbonated zones, often characterized by depleted calcium content and elevated carbon signals in the form of $CaCO_3$ deposits. For

conventional Portland systems, SEM–EDS frequently reveals progressive decalcification and disintegration of C–S–H gel, along with formation of expansive carbonation layers. In contrast, acid-resistant systems like CAPC or geopolymers exhibit denser, more uniform microstructures with distinct acid-stable phases such as hydroxyapatite or aluminosilicate networks, and minimal calcium leaching. SEM–EDS mapping is therefore indispensable for validating the chemical resilience of a cement matrix and understanding the spatial progression of degradation under acidic CO_2 exposure, bridging the gap between laboratory performance metrics and real-world geochemical behaviour (Mamoudou et al., 2023; Neves et al., 2025; Teodoriu and Bello, 2020).

4.3.4. pH buffering index

The pH Buffering Index is a critical parameter for evaluating the acid-neutralizing capacity of cement systems intended for CO_2 storage wells. It quantifies how effectively a cement matrix can resist acidification by consuming protons and stabilizing the pH of the surrounding environment—a key property in mitigating long-term degradation from carbonic acid (H_2CO_3) and associated in situ acids like H_2S and organic acids. This test typically involves finely ground, cured cement samples dispersed in deionized water or synthetic brine, followed by drop-wise titration with a standardized acid solution (e.g., 0.1 M HCl or CO_2-saturated brine), while continuously monitoring pH with a calibrated electrode.

The buffering capacity is calculated based on the volume of acid required to lower the pH from an initial value (typically ~11–12 for alkaline cement systems) to a critical pH threshold such as 4.0 or 3.5, which mimics the acidity of CO_2-saturated formation brine. Cement systems with strong buffering ability exhibit gradual pH decline, indicating the presence of stable alkaline phases (e.g., calcium aluminate hydrates, phosphate species, N-A-S-H gels) that can resist acid penetration. Conversely, systems rich in portlandite or unreacted lime show a rapid pH drop after initial neutralization, signalling vulnerability to leaching and breakdown. The pH buffering index thus complements immersion and mass loss tests by providing a dynamic view of chemical resilience and serves as a predictive tool for long-term cement durability in acidified CO_2 storage environments.

4.3.5. X-ray diffraction (XRD)

Phase identification in acid-resistant cement systems is a fundamental step in evaluating long-term performance, especially for CO_2 storage wells where exposure to carbonic acid and thermobaric conditions can destabilize conventional hydration products. The objective of this analysis is to confirm the presence of desired stable hydrates such as strätlingite (C_2ASH_8) in CAC-silica systems, N-A-S-H (sodium–aluminosilicate hydrate) gels in geopolymers, and hydroxyapatite ($Ca_5(PO_4)_3OH$) in phosphate-based binders while simultaneously ensuring the absence or minimal presence of deleterious phases like portlandite ($Ca(OH)_2$), which is highly vulnerable to leaching and carbonation in acidic environments (Chavez Panduro et al., 2017; Neves et al., 2024; Verba et al., 2017).

This is typically achieved using X-ray diffraction (XRD) combined with Rietveld refinement to quantify crystalline phase content. For amorphous or poorly crystalline phases such as C–S–H or N-A-S-H, complementary techniques like Fourier Transform Infrared Spectroscopy (FTIR), Raman spectroscopy, and Solid-State Nuclear Magnetic Resonance (NMR) are used to verify chemical structure and polymerization. The detection of strätlingite, for example, signifies improved acid durability due to its lower Ca/Si ratio and stable silicate framework. Similarly, hydroxyapatite formation in CAPC systems indicates phosphate fixation and acid neutralization potential, critical for resisting carbonic and organic acid attack. Conversely, detection of excessive portlandite, ettringite, or unstable aluminate hydrates like CAH_{10} suggests susceptibility to degradation, volume change, or sulphate-induced expansion (De Matos et al., 2022; Jupe et al., 2007).

The goal of this phase identification is not merely confirmation of hydration but to validate the intended chemical pathways of stability and predict durability under CO_2-rich environments. It also helps refine mix design strategies e.g., increasing silica fume for strätlingite formation or optimizing Na_2SiO_3/Al_2O_3 ratios in geopolymers to promote N-A-S-H gels—ensuring that the final cement matrix will resist acid attack while maintaining long-term mechanical and sealing integrity.

4.4. Phase IV – simulated zonal isolation & interface testing

The final phase simulates mechanical and hydraulic integrity under stress and flow conditions, assessing whether the cement can act as an effective long-term barrier.

4.4.1. Shear bond and tensile strength (Cement–casing interface)

Shear bond and tensile strength at the cement–casing interface are critical mechanical parameters that directly influence zonal isolation and long-term well integrity in CO_2 storage applications. These properties determine the cement's ability to adhere to steel casing under thermal, pressure, and chemical stress, especially during injection cycles and acid exposure. Poor bonding can lead to micro-annulus formation, CO_2 migration, and eventual loss of containment. These interfacial strengths are typically measured using push-out tests (for shear bond) or tensile pull tests, following procedures aligned with API RP 10B-3 or adapted from ASTM standards.

In the push-out test, a cement core cast inside a steel casing segment is subjected to axial loading until it is displaced, and the force required to break the bond is recorded. The tensile pull test uses a cement plug bonded to a steel plate or casing section, which is then pulled vertically until failure occurs at the interface. For both tests, samples are cured under reservoir-simulated conditions (e.g., 80–100 °C, up to 20 MPa), and optionally aged in CO_2-saturated brine to simulate field exposure. Acid-resistant cement systems such as CAC, CAPC, or geopolymer blends often demonstrate improved bonding due to low shrinkage, microstructural densification, and chemical interaction with steel (e.g., phosphate-based passivation) (Aman et al., 2018; Mahmoud and Elkatatny, 2020; Neves et al., 2025).

Post-acid exposure testing is especially crucial, as acidic conditions can degrade the interfacial transition zone by leaching calcium, weakening hydration products, and increasing permeability. A significant loss of shear or tensile strength after acid exposure signals poor long-term sealing potential, even if bulk compressive strength remains high. Therefore, interfacial strength testing is essential for validating the field readiness of any CO_2-well cementing system and ensures that both chemical durability and mechanical bonding are jointly optimized (Hwang et al., 2018; Li et al., 2020; Samarakoon et al., 2022; Sugama, 2006).

4.4.2. Gas/fluid migration test (annular flow simulation)

The Gas/Fluid Migration Test, often performed using a gas flow apparatus, is a specialized simulation designed to evaluate a cement system's ability to resist annular gas or fluid migration during its critical setting phase; a vulnerability window especially important for CO_2 storage wells. This test is particularly relevant for foamed, lightweight, or low-density acid-resistant systems, which may have inherently higher permeability and longer transition times from slurry to set. Gas migration during this window can lead to the formation of micro-annuli, loss of zonal isolation,

and premature CO_2 breakthrough ultimately compromising the long-term sealing function of the cement sheath (Al-Buraik et al., 1998; Al-Yami, 2015a; Checkai, 2012; Jennings et al., 2003).

In a typical setup, the slurry is placed in an annular mold or a specialized cylindrical cell, subjected to a controlled pressure differential that mimics downhole pore or gas pressure, and then allowed to set under reservoir-simulated temperature and pressure conditions (e.g., 80–100 °C and up to 20 MPa). As the cement slurry begins to thicken, compressed gas (often nitrogen or CO_2) is applied to the top or sides of the column. Any gas percolation through the setting cement is measured using flowmeters or pressure transducers, while the transition time (from slurry to gel and set) is recorded. Systems that allow gas to escape before fully setting are deemed to have poor static gel strength development and low migration resistance (Al-Yami et al., 2014).

For acid-resistant systems, this test also serves to validate how well the selected formulation maintains structural and sealing integrity under pressure-driven gas exposure. For instance, geopolymers and phosphate-based cements, with their rapid gelation and low permeability, often outperform conventional systems in migration resistance. Additionally, incorporation of nano-silica, latexes, or gas-blocking additives can significantly improve sealing performance. This test thus plays a pivotal role in optimizing slurry design to ensure early gas shut-off, particularly in CO_2 injection wells where immediate and lasting isolation is mission-critical (Al-Yami et al., 2010).

4.4.3. Permeability testing (Darcy flow or BCT)

Permeability testing, performed using either Darcy flow apparatus or Brine Conductivity Test (BCT), is essential for evaluating the sealing capacity of acid-resistant cement systems particularly before and after exposure to CO_2-rich fluids. Low permeability is a fundamental requirement for maintaining zonal isolation in CO_2 storage wells, where injected supercritical CO_2 or carbonic acid can exploit microchannels and degrade the matrix over time. The goal of this test is to determine whether the cement matrix maintains hydraulic integrity under simulated reservoir conditions and post-acid exposure (Griffith and Osisanya, 1999; Maharidge et al., 2016).

In a typical setup, cured cement plugs are mounted in a permeability cell and subjected to nitrogen gas or brine flow under controlled pressure gradients (usually 0.2–1 MPa), while flow rates are recorded to calculate permeability using Darcy's Law. In the Darcy gas flow method, nitrogen is often preferred due to its inertness and ease of measurement, whereas BCT is used to assess ionic transport pathways in saturated conditions. For CO_2 wells, the benchmark for effective sealing is typically <0.1 millidarcy (mD) values above this suggest microcracking, unhydrated pathways, or acid-induced matrix damage (Jain and Majumder, 2016; Wang et al., 2020).

Permeability is measured both before and after immersion in CO_2-saturated brine (e.g., pH ~3.5, 80–100 °C, 10–20 MPa) to assess degradation. Acid-resistant systems like CAPC, geopolymers, and CAC blends generally show minimal permeability changes post-exposure, due to formation of stable hydrates and acid-blocking phases like hydroxyapatite, N-A-S-H, or strätlingite. In contrast, traditional Portland cement often shows significant increases due to decalcification and pore coalescence. Thus, permeability testing provides a direct metric for evaluating the long-term sealing performance of cement systems in CO_2 storage applications, ensuring that both chemical durability and physical integrity are retained under aggressive conditions (Jafarzade, 2014; Plank, 2022).

4.4.4. Micro-CT scanning

Micro-Computed Tomography (Micro-CT) scanning is a powerful non-destructive technique that allows for high-resolution, three-dimensional visualization of the internal structure of cementitious materials making it particularly valuable for assessing acid-resistant cement systems in CO_2 storage well applications. Unlike surface-level characterization methods, Micro-CT provides a volumetric representation of internal porosity, microcrack formation, heterogeneity, and most importantly, depth of acid penetration after chemical exposure. This level of insight is critical in understanding the degradation pathways and performance limits of advanced cement formulations under real-world subsurface conditions (Børve, 2018).

In a typical workflow, cylindrical or prismatic cement samples are scanned both before and after immersion in CO_2-saturated brine (typically pH ~3.5, 80–100 °C, 10–20 MPa). The X-ray source penetrates the sample and captures thousands of 2D slices, which are then reconstructed into a 3D dataset. Specialized image analysis software can quantify changes in pore size distribution, pore connectivity, and crack volume, and can even differentiate chemically altered zones based on density variations such as decalcified, carbonated, or recrystallized regions. This allows researchers to map acid ingress depth and track how microstructural deterioration progresses over time (Bin Abed, 2024; Mamoudou et al., 2023; Skorpa et al., 2017).

For acid-resistant cements like CAPC, CAC-silica blends, or geopolymers, Micro-CT often reveals more uniform pore networks and minimal internal damage post-exposure, supporting the mechanical and chemical test findings. In contrast, conventional Portland systems typically exhibit greater internal porosity evolution and deeper acid penetration due to dissolution of Ca-rich phases. Therefore, Micro-CT scanning not only enhances the understanding of degradation mechanisms but also strengthens the case for adopting next-generation cements in long-duration CO_2 storage operations. When available, it serves as a gold-standard validation tool to correlate microstructural resilience with bulk performance metrics (Cao, 2014; Kirkland et al., 2019).

To complement Fig. 7, it is important to emphasize that each testing phase serves a distinct purpose. Phase I establishes baseline API parameters (slurry density, thickening time, compressive strength) to ensure operational compatibility. Phase II focuses on short-term chemical durability through controlled CO_2-brine exposure tests, where standardized indicators such as compressive strength retention, carbonation depth, and mass loss are quantified. Phase III extends to long-term durability under simulated reservoir P–T–pH conditions, with key metrics including permeability evolution, porosity change, and bond strength at casing–cement interfaces. Finally, Phase IV involves advanced tests such as cyclic injection simulation and microstructural analysis (SEM/EDS, XRD) to validate resistance under dynamic reservoir conditions. These programmed steps and key indicators provide a standardized framework that translates laboratory results into reliable predictions of field performance.

5. HSR screening criteria for cementing systems for CO_2 storage wells

The HSR screening criteria, an acronym for Hammad–Syahrir–Rajeswary, represents a comprehensive, multi-domain framework designed to evaluate and compare acid-resistant cement systems for CO_2 storage wells (see Fig. 8 and Table 7). Unlike conventional selection approaches that focus solely on mechanical strength or short-term durability, the HSR criteria integrate operational conditions, cement formulation performance, and sustainability constraints to provide a holistic evaluation of system suitability. It addresses critical reservoir realities such as elevated CO_2 partial pressures, thermobaric conditions, and brine chemistry, which drive aggressive degradation mechanisms like leaching, carbonation, and microcracking.

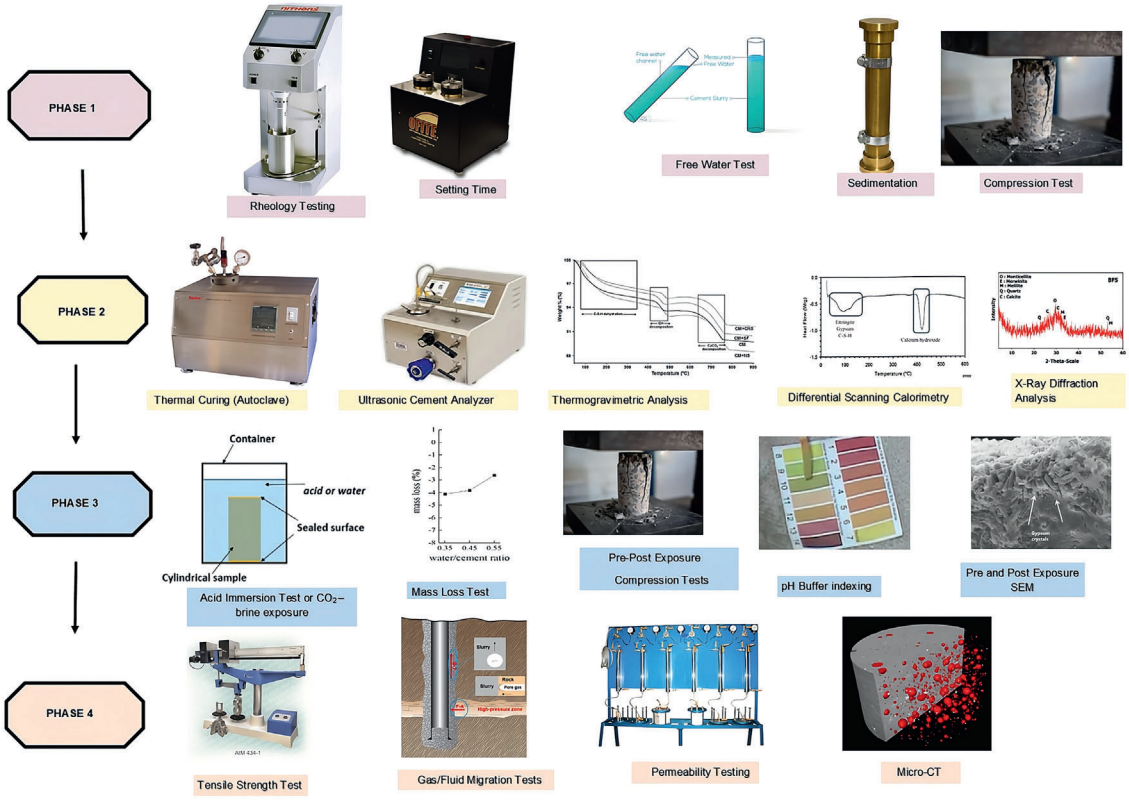

Fig. 7. Phase-wise API referred testing protocols for acid exposed cementing system.

Simultaneously, the framework mandates design benchmarks such as acid resistance indices, ion leaching rates, strength retention, and low permeability post-exposure to ensure long-term well integrity. By incorporating life-cycle CO_2 emissions, field readiness levels, and material toxicity, HSR also promotes responsible material innovation in alignment with global decarbonization goals. This screening matrix serves as a foundational tool for both lab-scale researchers developing novel cement systems and engineers tasked with qualifying these materials for deployment in critical carbon storage infrastructure.

The design of cementing systems for CO_2 storage wells must not be uniform across projects, as different reservoir types pose unique geochemical and geomechanical challenges that significantly impact cement durability. A tailored approach that aligns the cement chemistry, additive system, and microstructural characteristics with the specific conditions of each geological formation is essential to ensure long-term well integrity and CO_2 containment (see Fig. 9).

The proposed HSR decision matrix should be regarded as a conceptual screening framework rather than a fully developed computational tool. While it introduces quantitative benchmarks and weightings that enable structured comparisons across cement systems, it does not yet provide a fully algorithmic or automated workflow. The framework is intended to guide preliminary decision-making and highlight critical trade-offs, while its operationalization into software or field-deployable decision support tools remains an important direction for future work. By acknowledging this limitation, we position the HSR matrix as a first step toward bridging laboratory data with engineering practice, providing a foundation that can be refined into a more actionable tool in subsequent research.

In saline aquifers, the most widely targeted reservoirs for CO_2 sequestration, cement is exposed to brine saturated with dissolved CO_2, leading to the formation of carbonic acid with a pH typically in the range of 3–4. These formations often exhibit moderate temperatures (35–80 °C) and pressures (10–25 MPa). In such settings, conventional Portland cement is highly vulnerable due to rapid leaching of portlandite and decalcification of C–S–H phases. Therefore, cementing systems should prioritize acid-resistant binders such as calcium aluminate cement (CAC), geopolymers, or calcium aluminate phosphate cement (CAPC). These systems offer intrinsic chemical durability, form stable hydration products

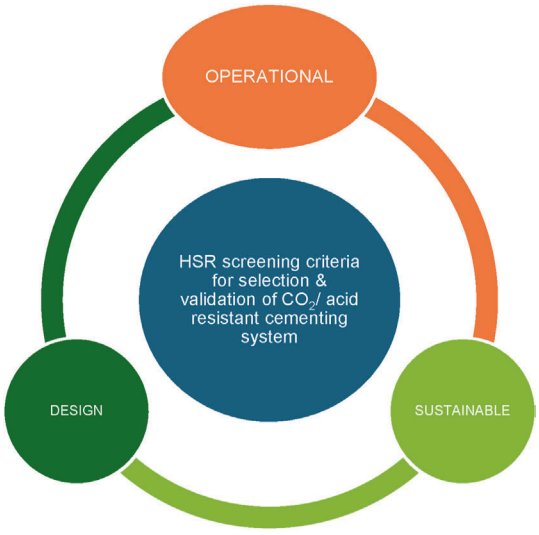

Fig. 8. HSR screening criteria for selection and validation of acid/CO_2-brine resistant systems named after its creators i.e., H=Hammad, S=Syahrir, R=Rajeswary.

Table 7
Summary of H.S.R. screening criteria.

Domain	Screening Parameter	Target/Benchmark	Remarks
Operational	CO_2 Partial Pressure	>2 MPa (typically 3–10 MPa for deep storage)	High CO_2 pressure leads to carbonic acid (H_2CO_3) formation, reducing pH and accelerating CH leaching and C–S–H degradation.
	Downhole Temperature	Greater than 120 °C	Class G cement strength and properties declines above 120 °C. Influences hydration kinetics and phase stability (e.g., CAC conversion, strength retrogression in Portland systems).
	Formation Pressure	10–30 MPa	Reflects in-situ confinement stress; affects mechanical integrity, porosity control, and bond strength.
	Brine Composition	Simulated 1.5 M NaCl + Ca^{2+}/Mg^{2+}; pH 3–4 after CO_2	Divalent ions affect durability via precipitation/dissolution reactions; realistic brine simulates in-situ chemical environment.
	Service Life Target	≥50 years (preferably >100 years)	Cement must withstand acid exposure over geological timescales to ensure safe CO_2 containment.
Design	Base Binder Type	Portland (Class G/H) or alternative (CAC, geopolymer)	Selection must reflect CO_2-resistance; Portland requires heavy pozzolanic modification; non-Portland may offer intrinsic durability.
	Acid Resistance Index	<5% mass loss in pH 3.5 carbonic brine (28–56 days)	Key metric for degradation; measures mass retention in real CO_2-brine systems, not HCl surrogates.
	pH Buffering Capacity	Maintain pH ±0.5 in CO_2-brine for 48–72 h	Demonstrates internal neutralization ability of cement; critical for CO_2 environments where pH control is essential.
	Ion Leaching Rate (Ca, Si, Al, P)	<1.5 mg/cm^2/day (each ion)	Directly reflects matrix breakdown; Ca^{2+}/Si^{4+} release indicates C–S–H dissolution, a primary failure path in carbonic environments.
	Early Compressive Strength (24 h)	≥3.5 MPa (UCA or crush test)	Needed to support casing and prevent gas migration during early setting; too fast = shrinkage risk.
	Strength Retention Post-Acid	≥80% after 28-day acid exposure	Assesses structural integrity under aggressive CO_2–brine attack; retention is more meaningful than initial strength alone.
	Permeability After Acid Exposure	≤0.1 mD	Reflects ability to maintain zonal isolation; increased permeability = risk of CO_2/brine migration and loss of containment.
	Shear Bond Strength (Steel–Cement)	≥3 MPa post-acid exposure	Ensures long-term casing integrity; acid degradation often causes micro-annulus or debonding issues.
Sustainability	Additive Safety & Toxicity	No carcinogenicity, no reactive vapours (e.g., phenols)	Must be field-safe and comply with ECHA/GHS regulations; field mixing must not expose workers to chronic hazards.
	Life-Cycle CO_2 Footprint	≤250 kg CO_2 eq./ton cementitious material	Ensures that material choice doesn't negate net CO_2 storage by contributing excessive embodied emissions.
	Field Readiness Level (TRL)	TRL ≥6 for deployment; TRL ≥3 for lab-stage systems	Ensures real-world applicability; distinguishes between proven field systems and early-stage experimental mixes.
	Cost-Performance Ratio	≤1.5 × cost of conventional Class G system	Premium must be justified by extended durability, minimal maintenance, and improved containment security.

(stratlingite or hydroxyapatite), and exhibit lower calcium ion leaching. Nano-silica or graphene oxide may further enhance resistance by densifying the matrix and reducing permeability.

In contrast, depleted gas reservoirs present a drier, lower brine saturation environment with high reservoir pressure and thermal gradients, particularly if subjected to prior production cycling. These reservoirs are prone to thermal cracking, micro-annulus formation, and pressure drawdown effects that challenge cement integrity more mechanically than chemically. Here, elasticity and shrinkage control become more important than extreme acid resistance. Modified Portland cement systems incorporating styrene-butadiene latex, polymer admixtures, or resin blends can accommodate thermomechanical stress while maintaining bonding. Hybrid formulations that combine CAC with elastomeric additives can offer a balanced solution in such fields.

Depleted oil reservoirs, particularly those with residual hydrocarbons and organic acids, introduce the risk of degradation not only from carbonic acid but also from dissolved organic species and sometimes H_2S. These conditions require cementing systems that can tolerate mixed-acid attack and fluctuating redox potential. CAPC formulations are especially advantageous due to their ability to immobilize Ca^{2+} and resist attack from both inorganic and organic acids. The use of fly ash or metakaolin as supplementary cementitious materials (SCMs) in Portland systems can also be considered, provided the acid exposure is moderate and early compressive strength is not the primary requirement.

In basaltic or volcanic formations, silicate-rich lithologies with magnesium-rich brines may lead to ion-exchange reactions that destabilize certain cement hydrates. High mobility of Mg^{2+} can induce secondary mineral precipitation and swelling. In such settings, magnesium phosphate cements (MPC) and low-Ca

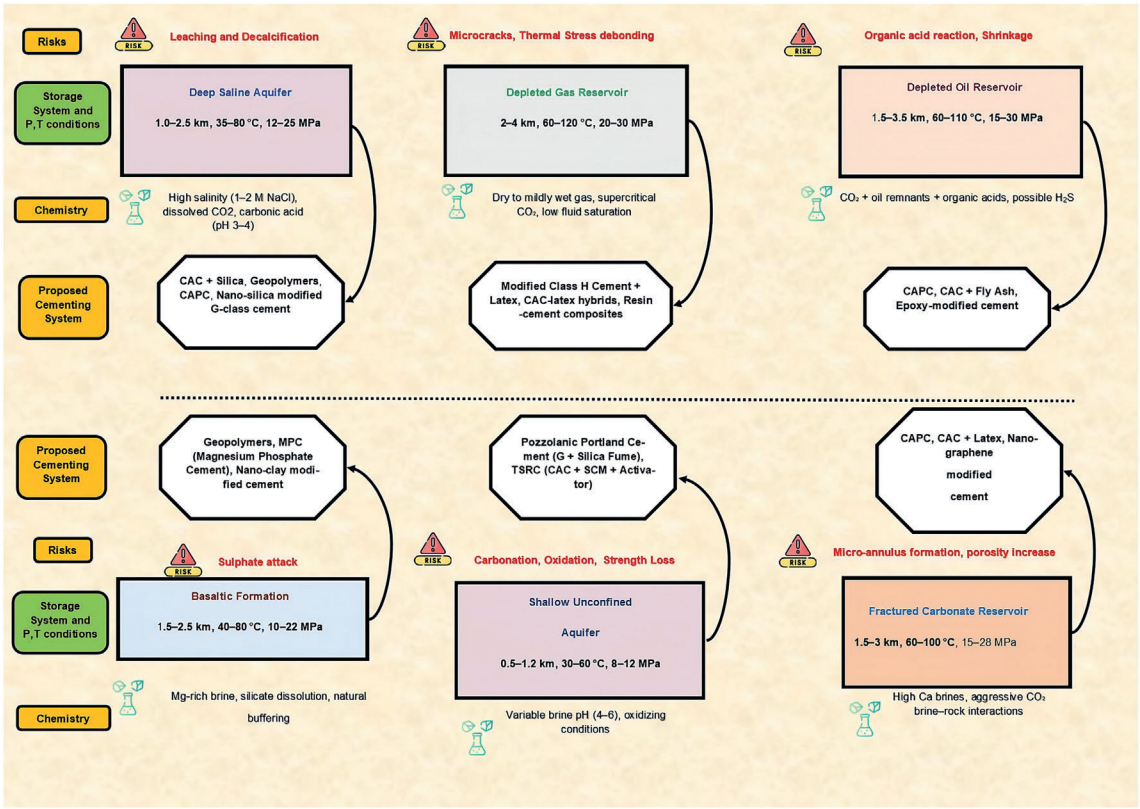

Fig. 9. Schematic overview of risks, reservoir chemistries, and proposed acid-resistant cementing systems across different CO_2 storage environments. Storage system pressure–temperature (P–T) conditions shown are averaged ranges derived from published reports and case studies. The figure highlights key degradation mechanisms (e.g., leaching, decalcification, sulphate attack, carbonation, micro-annulus formation), corresponding geochemical environments (e.g., dissolved CO_2, organic acids, Mg-rich brines, variable pH), and suitable cementing solutions (e.g., CAC, CAPC, MPC, geopolymers, resin-modified systems, nano-engineered composites).

geopolymers are preferable. These systems resist acid ingress, form stable struvite-like phases, and do not rely on portlandite, which is absent in their chemistry.

Lastly, in shallow aquifers or marginal formations, the CO_2 may not reach supercritical phase, but cement systems are still exposed to prolonged carbonated water exposure and atmospheric oxygen ingress. In such cases, cost-effective systems using Class G Portland cement modified with silica fume, fly ash, or nano-clays may be used, provided that sufficient testing confirms permeability control, adequate thickening time, and acid buffering capability. However, long-term monitoring and testing in representative synthetic brines is still required before field deployment.

Ultimately, a reservoir-specific cement design approach must be embedded into the CO_2 storage well planning process. Selection should not only be based on API classifications but must also reflect geochemistry, fluid saturation, thermal regime, and long-term chemical durability. Cement systems must be treated as a reactive barrier material, not merely a mechanical sealant, in the context of geologic CO_2 storage.

Fig. 9 is included as an illustrative demonstration of how the HSR framework can be applied in practice. Although the HSR matrix remains a conceptual screening tool at this stage, the figure translates its logic into a visual example that shows how cement systems can be comparatively ranked when benchmarked against defined performance thresholds. The purpose of Fig. 9 is not to present a finalized decision algorithm, but rather to demonstrate the potential utility of the framework in guiding material selection. In this way, it bridges the gap between purely qualitative descriptions and future quantitative decision-support tools, while also acknowledging that further refinement and field validation are required to make the HSR matrix fully operational.

6. Challenges and future perspectives

Based on this review some critical challenges have been identified, and a solid way forward has been outlined.

6.1. Key challenges

(1) Many acid-resistant systems, including polymer-modified Portland cements and nanomaterial-based systems, have shown promising short-term resistance to CO_2-brine environments. However, there is limited understanding of how these materials evolve over decades, especially under fluctuating temperature, pressure, and chemical conditions typical of deep saline aquifers and depleted reservoirs.
(2) Studies often use differing test durations, acid concentrations, curing conditions, and evaluation metrics (mass loss vs. strength retention), making it difficult to standardize performance comparison across cementing systems.
(3) Despite encouraging laboratory performance, most systems especially CAC, CAPC, geopolymers, and nanocomposites lack extensive real-well field validation under CO_2 injection and post-closure monitoring.
(4) Systems such as CAC are prone to hydrate conversion (e.g., $CAH_{10} \rightarrow C_3AH_6$) at elevated temperatures, leading to strength loss. Reliable mitigation strategies are still not universally agreed upon and need further optimization.

(5) High-grade CAC, phosphate binders, and nanomaterials like graphene oxide or CNTs are expensive or not readily available in bulk quantities. This raises concerns regarding scalability for full-well applications.
(6) Cement–brine interactions, especially in high Mg^{2+}, SO_4^{2-}, or Cl^- rich environments, remain poorly studied for several systems like CAPC and MPC, possibly altering cement stability over time.
(7) The environmental footprint of producing specialty cements and additives (e.g., phosphoric acid, latex polymers) is rarely quantified, limiting assessment of their suitability for long-term carbon-negative infrastructure.

6.2. Future research directions and roadmap

(1) Conduct long-duration (6–12 months or more) immersion experiments under SC-CO_2 brine conditions with standardized pressure (10–15 MPa) and temperature (60–90 °C) profiles to simulate real well environments. Emphasis should be placed on comparing strength retention, permeability, and carbonation depth.
(2) CAC systems need further real-well validation, especially under cyclic temperature and pressure conditions. For CAPC, dedicated field pilots must evaluate setting time control, phosphate leaching risk, and scale-up challenges, as well as mechanical bonding with casing and rock interfaces.
(3) A harmonized acid-resistance testing framework should be adopted across academia and industry. This includes standardizing parameters such as pH of exposure media, immersion duration, strength assessment intervals, and acid-neutralization index.
(4) Further research is needed on additives (e.g., silica fume, nano-silica, citric acid) that can retard or prevent strength retrogression in CAC systems under high-temperature curing. Thermo-chemical models should be integrated to predict hydrate evolution pathways.
(5) Combining CAC with CAPC or integrating nano-silica into geopolymer or MPC matrices could yield cementing systems with multi-modal resistance (thermal, chemical, and mechanical). Research should focus on blend ratios, compatibility, and synergistic hydration.
(6) Micro-CT and SEM imaging should be employed to study crack formation and interfacial debonding, particularly in high-pressure CO_2 zones. Cement–steel and cement–formation bonding under acid stress remains a critical knowledge gap.
(7) Conduct cradle-to-grave environmental and cost analysis of acid-resistant additives to determine the carbon and energy intensity of each system. This is essential for assessing their true value in carbon mitigation strategies.

7. Conclusions

The following conclusions can be drawn from this study.

(1) Portland cement systems are inherently vulnerable to CO_2-rich environments, primarily due to decalcification, carbonation, and leaching of calcium hydroxide, leading to strength loss, increased permeability, and long-term integrity failure.
(2) Non-Portland alternatives particularly CAC, CAPC, and MPC demonstrate superior chemical durability, with significantly lower carbonation depth and better retention of compressive strength after prolonged CO_2-brine exposure, making them promising candidates for high-risk CCS applications.
(3) Modified Portland systems (with pozzolans, latexes, polymers, and nanomaterials) can enhance acid resistance, but they remain transitional solutions with limited long-term reliability unless rigorously optimized and site-tailored.
(4) A structured phase-wise laboratory testing protocol and the HSR screening framework proposed in this study provide a practical roadmap for cement selection and validation, incorporating operational, chemical, and sustainability criteria aligned with API testing standards.
(5) A novel HSR screening tool is introduced that offers a holistic integration of operational parameters, sustainability, and reservoir-compatibility parameters to guide the selection and validation of durable cementing systems for CO_2 storage wells.
(6) Future research must prioritize systematic field trials and deeper mechanistic understanding of aluminate- and phosphate-based binders, especially under thermobaric and supercritical CO_2 conditions, to enable safe, long-duration zonal isolation for next-generation carbon storage projects.

Declaration of competing interest

The authors declare that they have no known competing financial interests or personal relationships that could have appeared to influence the work reported in this paper.

Acknowledgements

The authors would like to acknowledge Yayasan UTP-Prototype Research Grant No 015PBC-064.

Nomenclature

AFm	Alumino-Ferrite Monosulfate (monosulfate phase in hydrated cement)
AFt	Alumino-Ferrite Trisulfate (ettringite phase in hydrated cement)
API	American Petroleum Institute
CAC	Calcium Aluminate Cement
CAPC	Calcium Aluminate Phosphate Cement
CCS	Carbon Capture and Storage
CH	Calcium Hydroxide (Portlandite)
CO_2	Carbon Dioxide
C–S–H	Calcium Silicate Hydrate
C-A-S-H	Calcium Aluminosilicate Hydrate (gel in geopolymers)
CNT	Carbon Nanotube
GGBFS	Ground Granulated Blast-Furnace Slag
GO	Graphene Oxide
HPHT	High Pressure High Temperature
HSR	Hammad-Syahrir-Rajeswary (a screening framework introduced in this work)
MPC	Magnesium Phosphate Cement
N-A-S-H	Sodium Aluminosilicate Hydrate (gel in geopolymers)
pCO_2	Partial Pressure of Carbon Dioxide
sc-CO_2	Supercritical Carbon Dioxide
SEM	Scanning Electron Microscopy
TDS	Total Dissolved Solids

References

Agbasimalo, N., Radonjic, M., 2012. Experimental study of Portland cement/rock interface in relation to wellbore stability for carbon capture and storage (CCS). In: Proceedings of the 46th U.S. Rock Mechanics/Geomechanics Symposium. American Rock Mechanics Association, Chicago, Illinois, USA.
Aiken, T.A., Kwasny, J., Sha, W., Soutsos, M.N., 2018. Effect of slag content and activator dosage on the resistance of fly ash geopolymer binders to sulfuric

acid attack. Cem. Concr. Res. 111, 23–40.
Ajir, K., Toufigh, V., Ghaemian, M., 2025. Protecting ordinary cement concrete against acidic and alkaline attacks utilizing epoxy resin coating. Constr. Build. Mater. 472, 141003.
Akbulut, Z.F., Yavuz, D., Tawfik, T.A., Smarzewski, P., Guler, S., 2024. Enhancing concrete performance through sustainable utilization of Class-C and Class-F fly ash: a comprehensive review. Sustainability 16, 4905.
Al-Buraik, K., Al-Abdulqader, K., Bsaibes, R., 1998. Prevention of shallow gas migration through cement. In: Proceedings of the IADC/SPE Asia Pacific Drilling Technology Conference and Exhibition. Kuala Lumpur, Malaysia.
Al-Chaar, G.K., Alkadi, M., Yaksic, D.A., Kallemeyn, L.A., 2011. The Use of Natural Pozzolan in Concrete as an Additive or Substitute for Cement. U.S. Army Corps of Engineers, Engineer Research and Development Center, Construction Engineering Research Laboratory, Champaign, IL. ERDC/CERL TR-11-46.
Al-Khdheeawi, E.A., Vialle, S., Barifcani, A., Sarmadivaleh, M., Iglauer, S., 2018. Impact of injected water salinity on CO_2 storage efficiency in homogenous reservoirs. APPEA J 58, 44–50.
Al-Yami, A.S., 2015a. An innovative cement formula to mitigate gas migration problems in deep gas wells: lab studies and field cases. In: Proceedings of the SPE Kuwait Oil & Gas Show and Conference. Society of Petroleum Engineers, Mishref, Kuwait.
Al-Yami, A.S., 2015b. An overview of different chemicals used in designing cement slurries for oil and gas wells. In: Proceedings of the SPE Kuwait Oil & Gas Show and Conference. Society of Petroleum Engineers, Mishref, Kuwait.
Al-Yami, A., Schubert, J., Medina-Cetina, Z., Yu, O.-Y., 2010. Drilling expert system for the optimal design and execution of successful cementing practices. In: Proceedings of the IADC/SPE Asia Pacific Drilling Technology Conference and Exhibition. Society of Petroleum Engineers, Ho Chi Minh City, Vietnam.
Al-Yami, A., Wagle, W., Nasr-El-Din, H., Al-Humaidi, A., 2014. Cement formula to prevent gas migration problems in HT/HP wells. Int. J. Sci. Eng. Res. 5 (6), 1336–1342.
Al-Yami, A.S., Wagle, V., Mukherjee, T.S., Al-Badran, M., Aljubran, M., 2017. Consideration to batch mixing time improves API recommendation for testing cement slurries and prevents cement failures: lab testing and field application. In: Proceedings of the SPE Kingdom of Saudi Arabia Annual Technical Symposium and Exhibition. Society of Petroleum Engineers, Dammam, Saudi Arabia.
Ali, B., Abdelkader, B., Noureddine, B., Boualem, S., 2015. Numerical analysis of crack propagation in cement PMMA: application of SED approach. Struct. Eng. Mech. 55, 93–109.
Alias, N.S., Ridha, S., Yerikania, U., 2016. Effect of chemical EOR on class G oilwell cement integrity under elevated conditions. Procedia Eng. 148, 1066–1073.
Aman, M., Espinoza, D.N., Ilgen, A.G., Major, J.R., Eichhubl, P., Dewers, T.A., 2018. CO_2-induced chemo-mechanical alteration in reservoir rocks assessed via batch reaction experiments and scratch testing. Greenh. Gases Sci. Technol. 8, 133–149.
American Petroleum Institute, 1995. API 10A Specifications. Available at: https://www.saigaogroup.com/uploads/file/api-10a-standard.pdf.
Amiri, Y., Hassaninasab, S., Chehri, K., Zahedi, M., 2022. Investigating the effect of adding *Bacillus* bacteria and nano-clay on cement mortar properties. Case Stud. Constr. Mater. 17, e01167.
Anagnostopoulos, C.A., Sapidis, G., Papastergiadis, E., 2016. Fundamental properties of epoxy resin-modified cement grouts. Constr. Build. Mater. 125, 184–195.
Ansarizadeh, M., Dodds, K., Gurpinar, O., Pekot, L.J., Kalfa, Ü., Sahin, S., Uysal, S., Ramakrishnan, T., Sacuta, N., Whittaker, S., 2015. Carbon dioxide—challenges and opportunities. Oilfield Rev. 27, 36–50.
Arbad, N., Rincon, F., Teodoriu, C., Amani, M., 2021. Experimental investigation of deterioration in mechanical properties of oil-based mud contaminated API cement slurries and correlations for ultrasonic cement analysis. J. Pet. Sci. Eng. 205, 108909.
Arora, A., Singh, B., Kaur, P., 2019. Novel material—magnesium phosphate cement (MPC) as repairing material in roads and buildings. Mater. Today Proc. 17, 70–76.
Arshad, M.T., Ahmad, S., Khitab, A., Hanif, A., 2021. Synergistic use of fly ash and silica fume to produce high-strength self-compacting cementitious composites. Crystals 11, 915.
Ashraf, S., Bogaerts, M., Mohanaraju, H., 2024. Impact of silica blend towards early compressive strength development of well cement class G. In: Proceedings of the Offshore Technology Conference Asia (OTC Asia). Offshore Technology Conference. Kuala Lumpur, Malaysia.
Bachu, S., 2015. Review of CO_2 storage efficiency in deep saline aquifers. Int. J. Greenh. Gas Control 40, 188–202.
Bachu, S., Bennion, D.B., 2009. Experimental assessment of brine and/or CO_2 leakage through well cements at reservoir conditions. Int. J. Greenh. Gas Control 3, 494–501.
Bai, M., Zhang, Z., Fu, X., 2016. A review on well integrity issues for CO_2 geological storage and enhanced gas recovery. Renew. Sustain. Energy Rev. 59, 920–926.
Baldissera, A.F., Schütz, M.K., dos Santos, L.M., Vecchia, F.D., Seferin, M., Ligabue, R., Costa, E.M., Chaban, V.V., Menezes, S.C., Einloft, S., 2017. Epoxy resin–cement paste composite for wellbores: evaluation of chemical degradation fostered by carbon dioxide. Greenh. Gases Sci. Technol. 7, 1065–1079.
Bannister, C.E., 1980. Rheological evaluation of cement slurries: methods and models. In: Proceedings of the SPE Annual Technical Conference and Exhibition. Society of Petroleum Engineers, Dallas, Texas, USA.
Barlet-Gouédard, V., Rimmelé, G., Goffé, B., Porcherie, O., 2007. Well technologies for CO_2 geological storage: CO_2-resistant cement. Oil Gas Sci. Technol. – Rev. IFP 62, 325–334.
Barlet-Gouédard, V., Rimmelé, G., Porcherie, O., Quisel, N., Desroches, J., 2009. A solution against well cement degradation under CO_2 geological storage environment. Int. J. Greenh. Gas Control 3, 206–216.
Batista, G.S., Takimi, A.S., Costa, E.M., 2024. Chemical changes in the composition of oil well cement with core/shell nanoparticle addition under CO_2 geological storage conditions. Energy Fuels 38, 22947–22958.
Bayuaji, R., Yasin, A.K., Susanto, T.E., Darmawan, M.S., 2017. A review in geopolymer binder with dry mixing method (geopolymer cement). In: AIP Conference Proceedings, vol. 1887. American Institute of Physics, Melville, NY, USA, 020001.
Beltrame, N.A.M., Medeiros-Junior, R.A., Dias, R.L., Witzke, F.B., 2023. Preliminary study of the effect of carbonation curing on geopolymers. Rev. IBRACON Estrut. Mater. 17, e17110.
Bertron, A., 2012. Methods for testing cementitious materials exposed to organic acids. In: Performance of Cement-based Materials in Aggressive Aqueous Environments: State-Of-The-Art Report, RILEM TC 211-PAE. Springer, pp. 355–387.
Bertron, A., Duchesne, J., Escadeillas, G., 2005. Attack of cement pastes exposed to organic acids in manure. Cem. Concr. Compos. 27, 898–909.
Bertron, A., Duchesne, J., Escadeillas, G., 2007. Degradation of cement pastes by organic acids. Mater. Struct. 40, 341–354.
Bett, E., 2017. Geothermal Well Cementing, Materials and Placement Techniques. LAP LAMBERT Academic Publishing.
Bin Abed, A., 2024. Investigation on Wellbore Cement Integrity During Carbon Capture and Storage (CCS) and Underground Hydrogen Storage (UHS). MSc Thesis. Texas A&M University, USA.
Binti Sauki, A., Irawan, S., 2010. Effects of pressure and temperature on well cement degradation by supercritical CO_2. Int. J. Eng. Technol. (IJET-IJENS) 10 (4), 22–28.
Blount, C.G., Brady, J.L., Fife, D.M., Gantt, L.L., Heusser, J.M., Hightower, M.C., 1991. HCl/HF acid-resistant cement blend: model study and field application. J. Pet. Technol. 43, 226–232.
Bogue, R.H., 1955. The Chemistry of Portland Cement, second ed. Reinhold Publishing Corporation, New York.
Boodaghians, R., 1998. Cross-linking acrylic cement mixture. Surf. Coat. Int. 81, 610–614.
Børve, I., 2018. In-situ μ-CT of Well Cement Exposed to CO_2-saturated Water at High Pressure and Temperature (Phd Thesis). Norwegian University of Science and Technology (NTNU), Trondheim, Norway.
Camacho, M.C., Galao, O., Baeza, F.J., Zornoza, E., Garcés, P., 2014. Mechanical properties and durability of CNT cement composites. Materials 7, 1640–1651.
Cao, P., 2014. Investigation of Cement Alteration and Associated Conductivity Change in CO_2-rich Environments Relevant to Carbon Sequestration (Phd Thesis). Pennsylvania State University, USA.
Carde, C., Francois, R., 1999. Modelling the loss of strength and porosity increase due to the leaching of cement pastes. Cem. Concr. Compos. 21, 181–188.
Carey, J.W., 2013. Geochemistry of wellbore integrity in CO_2 sequestration: portland cement–steel–brine–CO_2 interactions. Rev. Mineral. Geochem. 77, 505–539.
Carroll, S., Carey, J.W., Dzombak, D., Huerta, N.J., Li, L., Richard, T., Um, W., Walsh, S. D., Zhang, L., 2016. Role of chemistry, mechanics, and transport on well integrity in CO_2 storage environments. Int. J. Greenh. Gas Control 49, 149–160.
Cestari, A.R., Vieira, E.F., Alves, F.J., Silva, E.C., Andrade Jr, M.A., 2012. A novel and efficient epoxy/chitosan cement slurry for use in severe acidic environments of oil wells—Structural characterization and kinetic modeling. J. Hazard. Mater. 213, 109–116.
Chavez Panduro, E., Torsæter, M., Gawel, K., Bjørge, R., Gibaud, A., Yang, Y., Bruns, S., Zheng, Y., Sørensen, H., Breiby, D., 2017. In-situ X-ray tomography study of cement exposed to CO_2-saturated brine. Environ. Sci. Technol. 51, 9344–9351.
Chavez Panduro, E.A., Cordonnier, B., Gawel, K., Børve, I., Iyer, J., Carroll, S.A., Michels, L., Rogowska, M., McBeck, J.A., Sørensen, H.O., 2020. Real-time 3D observations of Portland cement carbonation at CO_2 storage conditions. Environ. Sci. Technol. 54, 8323–8332.
Checkai, D.A., 2012. Estimating Permeability Distribution of Leakage Pathways Along Existing Wellbores. M.S. Thesis. The University of Texas at Austin, USA.
Chen, J.J., Thomas, J.J., Jennings, H.M., 2006. Decalcification shrinkage of cement paste. Cem. Concr. Res. 36, 801–809.
Chen, S., Collins, F.G., MacLeod, A.J.N., Pan, Z., Duan, W., Wang, C.M., 2011. Carbon nanotube–cement composites: a retrospect. IES J. Part A: Civ. Struct. Eng. 4, 254–265.
Chen, X., Wang, C., Xue, Y., Chen, Z., Jin, J., Wang, R., 2021. A novel thermo-thickening viscosity-modifying admixture to improve settlement stability of cement slurry under high temperatures. Constr. Build. Mater. 295, 123606.
Cheng, B., Yao, C., Xiong, J., Liu, X., Zhang, H., Zhang, S., 2020. Effects of sodium hexametaphosphate addition on the dispersion and hydration of pure calcium aluminate cement. Materials 13, 5229.
Choi, Y.-S., Young, D., Nešić, S., Gray, L.G., 2013. Wellbore integrity and corrosion of carbon steel in CO_2 geologic storage environments: a literature review. Int. J. Greenh. Gas Control 16 (Suppl. l.), S70–S77.
Chotard, T., Gimet-Breart, N., Smith, A., Fargeot, D., Bonnet, J., Gault, C., 2001. Application of ultrasonic testing to describe the hydration of calcium aluminate cement at early age. Cem. Concr. Res. 31, 405–412.
Chuah, S., Pan, Z., Sanjayan, J.G., Wang, C.M., Duan, W.H., 2014. Nano-reinforced cement and concrete composites and new perspective from graphene oxide.

Constr. Build. Mater. 73, 113–124.
Çolak, A., 2005. Properties of plain and latex-modified Portland cement pastes and concretes with and without superplasticizer. Cem. Concr. Res. 35, 1510–1521.
Consoli, N.C., Quiñónez Samaniego, R.A., González, L.E., Bittar, E.J., Cuisinier, O., 2018. Impact of severe climate conditions on loss of mass, strength, and stiffness of compacted fine-grained soils–Portland cement blends. J. Mater. Civ. Eng. 30, 04018174.
Costa, B., Freitas, J., Araujo, R., Oliveira, Y., Santiago, R., Oliveira, F., 2021. Analysis of different oil well cement slurry formulations exposed to a CO_2-rich environment. J. CO_2 Util. 51, 101636.
Damion, T., Chaunsali, P., 2022. Evaluating acid resistance of Portland cement, calcium aluminate cement, and calcium sulfoaluminate-based cement using acid neutralisation. Cem. Concr. Res. 162, 107000.
De Matos, P., Neto, J.A., Sakata, R., Kirchheim, A., Rodríguez, E., Campos, C., 2022. Strategies for XRD quantitative phase analysis of ordinary and blended Portland cements. Cem. Concr. Compos. 131, 104571.
Defus, A., Possenti, E., Sansonetti, A., Tedeschi, C., Colombo, C., Biondelli, D., Vettori, S., Realini, M., 2021. Di-ammonium hydrogen phosphate for the consolidation of lime-based historic mortars – preliminary research. J. Cult. Herit. 48, 45–53.
Dembovska, L., Bajare, D., Pundiene, I., Vitola, L., 2017. Effect of pozzolanic additives on the strength development of high-performance concrete. Procedia Eng. 172, 202–210.
Dinesh, K., Sonny, I., Syahrir, R., Davannendran, C., Nuriman, A., 2018. The suitability of fly-ash-based geopolymer cement for oil well cementing applications: a review. ARPN J. Eng. Appl. Sci. 13, 8296–8306.
Doan, A.A., Holley, A.C., Li, L., Kellum, M.G., 2017. A novel cement system to ensure slurry stability in a horizontal well. In: Proceedings of the SPE Oklahoma City Oil and Gas Symposium. Society of Petroleum Engineers, Oklahoma City, USA.
Duguid, A., Scherer, G.W., 2010. Degradation of oilwell cement due to exposure to carbonated brine. Int. J. Greenh. Gas Control 4, 546–560.
Duguid, A., Radonjic, M., Scherer, G.W., 2011. Degradation of cement at the reservoir/cement interface from exposure to carbonated brine. Int. J. Greenh. Gas Control 5, 1413–1428.
Enick, R.M., Klara, S.M., 1990. CO_2 solubility in water and brine under reservoir conditions. Chem. Eng. Commun. 90, 23–33.
Evju, C., Hansen, S., 2001. Expansive properties of ettringite in a mixture of calcium aluminate cement, Portland cement and β-calcium sulfate hemihydrate. Cem. Concr. Res. 31, 257–261.
Falode, O., Salam, K., Arinkoola, A., Ajagbe, B., 2013. Prediction of compressive strength of oil-field Class G cement slurry using factorial design. J. Pet. Explor. Prod. Technol. 3, 297–302.
Fan, L., Xu, F., Wang, S., Yu, Y., Zhang, J., Guo, J., 2023. A review on the modification mechanism of polymer on cement-based materials. J. Mater. Res. Technol. 26, 5816–5837.
Fikeni, K.G., Pang, X., Yu, Y., Xia, X., Sun, F., Wang, H., Lv, K., Sun, J., 2024. An overview of oil well cement retarders and the retardation mechanisms. Geoenergy Sci. Eng., 213116
Gandelman, R., Miranda, C., Teixeira, K., Martins, A.L., Waldmann, A., 2004. On the rheological parameters governing oilwell cement slurry stability. Annu. Trans. Nordic Rheol. Soc. 12, 85–91.
García-Lodeiro, I., Fernández-Jiménez, A., Palomo, A., 2013. Variation in hybrid cements over time: alkaline activation of fly ash–Portland cement blends. Cem. Concr. Res. 52, 112–122.
Gaurina-Međimurec, N., 2010. The influence of CO_2 on well cement. Rudarsko-Geolosko-Naftni Zb. 22, 19–25.
Gaurina-Međimurec, N., Pašić, B., Mijić, P., Medved, I., 2021. Drilling fluid and cement slurry design for naturally fractured reservoirs. Appl. Sci. 11, 767.
Gawlicki, M., Nocuń-Wczelik, W., Bąk, Ł., 2010. Calorimetry in the studies of cement hydration: setting and hardening of Portland cement–calcium aluminate cement mixtures. J. Therm. Anal. Calorim. 100, 571–576.
Ghassemi, P., Toufigh, V., 2020. Durability of epoxy polymer and ordinary cement concrete in aggressive environments. Constr. Build. Mater. 234, 117887.
Glasser, F.P., Luke, K., Angus, M., 1988. Modification of cement pore fluid compositions by pozzolanic additives. Cem. Concr. Res. 18, 165–178.
Gowthaman, S., Krishnya, S., Nasvi, M., 2016. Effect of salinity on mechanical behaviour of well cement: application to carbon capture and storage wells. Engineer: J. Inst. Eng. Sri Lanka 49 (1), 35–44.
Griffith, J., Osisanya, S., 1999. Effect of drilling fluid filter cake thickness and permeability on cement slurry fluid loss. J. Can. Pet. Technol. 38 (13), 36–41.
Gruber, S., Plank, J., 2020. Preparation and effectiveness of a high-temperature anti-settling agent for well cement slurries. J. Nat. Gas Sci. Eng. 81, 103416.
Guo, J., Pan, W., Fan, J., Yu, Y., 2018. Improving the performance of oilwell cement by graft-modified PB latex. Trans. Tianjin Univ. 24, 434–441.
Haagsma, A., Weber, S., Moody, M., Sminchak, J., Gerst, J., Gupta, N., 2017. Comparative wellbore integrity evaluation across a complex of oil and gas fields within the Michigan Basin and implications for CO_2 storage. Greenh. Gases Sci. Technol. 7, 828–842.
Haider, M.G., 2014. Investigation of Geopolymer as an Alternative Cementing Material for Wellbore Applications (Phd Thesis). Swinburne University of Technology, Melbourne, Australia.
Hatungimana, D., Yazici, Ş., Orhan, Ş., Mardani-Aghabaglou, A., 2020. Effect of styrene-butadiene copolymer (SBR) latex on mechanical and transport properties of Portland cement mortar. J. Green Build. 15, 185–197.
Herfort, D., Moir, G., Johansen, V., Sorrentino, F., Arceo, H.B., 2010. The chemistry of Portland cement clinker. Adv. Cem. Res. 22, 187–194.
Hodne, H., Saasen, A., O'Hagan, A.B., Wick, S.O., 2000. Effects of time and shear energy on the rheological behaviour of oilwell cement slurries. Cem. Concr. Res. 30, 1759–1766.
Huang, H., Qian, C., Zhao, F., Qu, J., Guo, J., Danzinger, M., 2016. Improvement on microstructure of concrete by polycarboxylate superplasticizer (PCE) and its influence on durability of concrete. Constr. Build. Mater. 110, 293–299.
Huo, J.-h., Yu, B.-s., Peng, Z.-g., Wu, Z.-s., Zhang, L.-h., 2021. Thermal control effects and mechanism of slag and fly ash on heat development of cement slurry used in hydrate formation. J. Nat. Gas Sci. Eng. 91, 103967.
Hussain, A., 2021. Designing a cost-effective Ultra-lightweight high-strength Cement Slurry for Intermediate Casing in the Permian Basin (Phd Dissertation. Texas Tech University, Lubbock, USA.
Hwang, J., Ahmed, R., Tale, S., Shah, S., 2018. Shear bond strength of oil well cement in carbonic acid environment. J. CO_2 Util. 27, 60–72.
Irico, S., De Meyst, L., Qvaeschning, D., Alonso, M.C., Villar, K., De Belie, N., 2020. Severe sulfuric acid attack on self-compacting concrete with granulometrically optimized blast-furnace slag—comparison of different test methods. Materials 13, 1431.
Iyengar, S., Al-Tabbaa, A., 2007. Developmental study of a low-pH magnesium phosphate cement for environmental applications. Environ. Technol. 28, 1387–1401.
Jafarzade, G., 2014. Leakage of CO_2 Along Annular Well Cement (Phd Thesis). Norwegian University of Science and Technology (NTNU), Trondheim, Norway.
Jahanbakhsh, A., Liu, Q., Hadi Mosleh, M., Agrawal, H., Farooqui, N.M., Buckman, J., Recasens, M., Maroto-Valer, M., Korre, A., Durucan, S., 2021. An investigation into CO_2–brine–cement–reservoir rock interactions for wellbore integrity in CO_2 geological storage. Energies 14, 5033.
Jain, A., Majumder, R., 2016. Strength, permeability and carbonation properties of concrete containing Kota stone slurry. Int. J. 4 (4), 735–739.
Jaishankar, P., Karthikeyan, C., 2017. Characteristics of cement concrete with nano alumina particles. IOP Conf. Ser. Earth Environ. Sci. 80 (1), 012005.
Jani, P., Imqam, A., 2021. Class C fly ash-based alkali-activated cement as a potential alternative cement for CO_2 storage applications. J. Pet. Sci. Eng. 201, 108408.
Japan Society of Civil Engineers, 2010. 2009 "Technology Summary" for Innovative Technique Award. Japan Society of Civil Engineers, 2010. Available at: https://www.jsce.or.jp/committee/concrete/e/newsletter/newsletter24/index_files/techaward.htm.
Jayakumari, B.Y., Swaminathan, E.N., Partheeban, P., 2023. A review on characteristics studies on carbon nanotubes-based cement concrete. Constr. Build. Mater. 367, 130344.
Jennings, S.S., Al-Ansari, A.A., Al-Yami, A.S., 2003. Gas migration after cementing greatly reduced. In: Proceedings of the SPE Middle East Oil and Gas Show & Conference. Society of Petroleum Engineers, Bahrain. Paper SPE-81414-MS.
Joel, O., Ademiluyi, F., 2011. Modelling of compressive strength of cement slurry at different slurry weights and temperatures. Res. J. Chem. Sci. 1, 128–134.
John, S.K., Nadir, Y., Cascardi, A., Arif, M.M., Girija, K., 2023. Effect of addition of nanoclay and SBR latex on fly ash-slag geopolymer mortar. J. Build. Eng. 66, 105875.
Jupe, A.C., Wilkinson, A.P., Luke, K., Funkhouser, G.P., 2007. Slurry consistency and in-situ synchrotron X-ray diffraction during early hydration of Portland cements with calcium chloride. J. Am. Ceram. Soc. 90, 2595–2602.
Kanesan, D., Ridha, S., Rao, P., 2017. Formulation of geopolymer cement using mixture of slag and Class F fly ash for oil well cementing. IOP Conf. Ser. Mater. Sci. Eng. 201, 012014. IOP Publishing, Bristol, UK.
Kang, Z., Zhang, J., Hou, D., Dong, B., 2023. Effects of tannic acid on the late-age strength of autoclave curing cement paste. Constr. Build. Mater. 390, 131740.
Karakaya, G., Kök, M., 2013. A study to determine the cement slurry behaviour to prevent the fluid migration. In: Proceedings of the 19th International Petroleum & Natural Gas Congress and Exhibition of Turkey. Istanbul, Turkey.
Kharaka, Y.K., Thordsen, J.J., Hovorka, S.D., Nance, H.S., Cole, D.R., Phelps, T.J., Knauss, K.G., 2009. Potential environmental issues of CO_2 storage in deep saline aquifers: geochemical results from the Frio-I Brine Pilot test, Texas, USA. Appl. Geochem. 24, 1106–1112.
Kirkland, C.M., Norton, D., Firth, O., Eldring, J., Cunningham, A.B., Gerlach, R., Phillips, A.J., 2019. Visualizing MICP with X-ray μ-CT to enhance cement defect sealing. Int. J. Greenh. Gas Control 86, 93–100.
Konduru, S.K.R., 2009. Performance Evaluations of latex-modified and Silica Fume Modified Concrete Overlays for Bridge Decks (M.S. Thesis). West Virginia University, Morgantown, USA.
Kremieniewski, M., Rzepka, M., Stryczek, S., Wiśniowski, R., 2017. The influence of anti-sedimentation agents on the technological parameters of cement slurry. AGH Drill. Oil Gas 34 (4), 945.
Krishnaveni, C., Selvan, S.S., 2021. Study on nano-alumina in concrete. Mater. Today Proc. 46, 3648–3652.
Krueger, R.F., 1986. An overview of formation damage and well productivity in oilfield operations. J. Pet. Technol. 38, 131–152.
Kutchko, B.G., Strazisar, B.R., Lowry, G.V., Dzombak, D.A., Thaulow, N., 2008. Rate of CO_2 attack on hydrated Class H well cement under geologic sequestration conditions. Environ. Sci. Technol. 42, 6237–6242.
Kutchko, B.G., Strazisar, B.R., Hawthorne, S.B., Lopano, C.L., Miller, D.J., Hakala, J.A., Guthrie, G.D., 2011. H_2S–CO_2 reaction with hydrated Class H well cement: Acid-gas injection and CO_2 co-sequestration. Int. J. Greenh. Gas Control 5, 880–888.

Lanabi, H., 2024. Carbon Capture and Storage in Algeria. University of Ouargla, Algeria. Available at: https://dspace.univ-ouargla.dz/jspui/bitstream/123456789/37210/1/HanineLanabi.pdf.
Langan, B., Weng, K., Ward, M., 2002. Effect of silica fume and fly ash on heat of hydration of Portland cement. Cem. Concr. Res. 32, 1045–1051.
Lesti, M., Tiemeyer, C., Plank, J., 2013. CO_2 stability of portland-cement-based well cementing systems for use on carbon capture & storage (CCS) wells. Cem. Concr. Res. 45, 45–54.
Li, Y., Ahmed, R., Han, B., Lu, Y., Jin, Y., 2020. Chemo-mechanical composite layer model for CO_2-attacked cement. Constr. Build. Mater. 252, 119128.
Liu, H., Bu, Y., Tian, L., Lu, C., 2018. Suitability of amphoteric ion polymer as retarder for calcium aluminate phosphate cement. In: ISOPE Int. Ocean and Polar Eng. Conf. [conference paper].
Liu, H., Bu, Y., Ma, R., Guo, W., 2019. Improve the practicability of calcium aluminate phosphate cement as well cement: application of amphoteric ion polymer as retarder. Constr. Build. Mater. 199, 207–213.
Liu, G., Kan, D., Cao, S.C., Chen, Z., Lyu, Q., 2022. Effect of multi-walled carbon nanotube on reactive powder concrete performance in sulfate dry–wet cycling environment. Constr. Build. Mater. 342, 128075.
Lota, J., Farris, S., Luke, K., 2013. API standard Class G cement and its inconsistencies in slurry thickening times. In: 35th International Conference on Cement Microscopy.
Lv, K., Huang, Z., Ling, X., Xia, X., 2022. Analysis of the weight loss of high temperature cement slurry. Fluid Dyn. Mater. Process. 18, 1307–1318.
Ma, R., Wang, Y., Li, H., Bai, Y., 2023. Progress in the polycarboxylate superplasticizer and their structure–activity relationship – a review. Mater. Today Commun. 35, 105838.
Maharidge, R., Bottiglieri, A., Dighe, S., Holley, A., Zhang, H., Koch, A., 2016. Development of permeability and mechanical properties of Class G cement from slurry to set. In: Proceedings of the SPE Annual Technical Conference and Exhibition. UAE, Dubai.
Mahmoud, A.A.A., 2020. Development of oil-well Cement Formulations for CO2-rich Environment Relevant to Geologic Carbon Sequestration (PhD Dissertation). King Fahd University of Petroleum & Minerals (KFUPM), Dhahran, Saudi Arabia.
Mahmoud, A.A., 2024a. Critical evaluation of API free-water test addressing gaps in lightweight cement slurries testing. In: Proceedings of ADIPEC 2024 (Abu Dhabi Int. Petroleum Exhibition and Conference). Abu Dhabi, United Arab Emirates.
Mahmoud, A.A., 2024b. Reassessing free-water API testing procedure. In: Proceedings of the SPE Annual Technical Conference and Exhibition. New Orleans, Louisiana, USA.
Mahmoud, A.A., Elkatatny, S., 2020. Improved durability of Saudi Class G oil-well cement sheath in CO_2-rich environments using olive waste. Constr. Build. Mater. 262, 120623.
Mamoudou, S., Curtis, M., Dang, S., Rai, C., Sondergeld, C., 2023. Experimental evaluation of cement integrity on exposure to CO_2: application to geostorage. In: Proceedings of the. SPE/AAPG/SEG Unconventional Resources Technology Conference, Denver, Colorado, USA. Paper URTEC-3864823-MS.
Martín, C.M., Ghabezloo, S., Piqué, T.M., Pereira, J.-M., Manzanal, D.G., 2023. Lightweight cement pastes with hollow glass microspheres: analytical estimation of elastic parameters. Cem. Concr. Res. 172, 107200.
Matteo, E.N., Scherer, G.W., 2012. Experimental study of the diffusion-controlled acid degradation of Class H Portland cement. Int. J. Greenh. Gas Control 7, 181–191.
Mohammed, A., Mahmood, W., Ghafor, K., 2020. TGA, rheological properties with maximum shear stress and compressive strength of cement-based grout modified with polycarboxylate polymers. Constr. Build. Mater. 235, 117534.
Mozaffari, S., Rahmani, O., Piroozian, A., Ziabakhsh-Ganji, Z., Mostafavi, H., 2022. Oil-well lightweight cement slurry for improving compressive strength and hydration rate in low-temperature conditions. Constr. Build. Mater. 357, 129301.
Mueller, D.T., 2012. Deepwater cementing standards: applicability and regulatory impact of best practices. In: Proceedings of the Offshore Technology Conference. Offshore Technology Conference. Houston, Texas, USA. Paper OTC-21735-MS.
Murtaza, M., Rahman, M.K., Al-Majed, A.A., 2016. Effect of nanoclay on mechanical and rheological properties of oil-well cement slurry under HPHT environment. In: Proceedings of the International Petroleum Technology Conference. Society of Petroleum Engineers, Bangkok, Thailand. Paper IPTC-18989-MS.
Naik, T.R., Singh, S.S., Ramme, B.W., 2001. Performance and leaching assessment of flowable slurry. J. Environ. Eng. 127, 359–368.
Nascimento, J.D., Rocha, C.A.A., Simão, C.A., Toledo Filho, R.D., 2022. Behavior of oil well cement slurry systems aged in CO_2-saturated water under high pressure and temperature. J. Therm. Anal. Calorim. 1–13.
Nasvi, M., Ranjith, P., Sanjayan, J., 2012. Comparison of mechanical behaviors of geopolymer and Class G cement as well cement at different curing temperatures for geological sequestration of carbon dioxide. In: ARMA U.S. Rock Mechanics/Geomechanics Symposium.
Nath, F., Mahmood, M.N., Yousuf, N., 2024. Recent advances in CCUS: a critical review on technologies, regulatory aspects and economics. Geoenergy Sci. Eng., 212726
Neves, A.V., Lima, V.N., Lima, I.N., Letichevsky, S., de Avillez, R.R., de Andrade Silva, F., 2024. The influence of H_2S and CO_2 on the triaxial behavior of Class G cement paste under elevated temperature and pressure. Geoenergy Sci. Eng. 240, 213084.
Neves, A.V., Lima, V.N., de Andrade Silva, F., 2025. Effects of brine and CO_2 exposure on the mechanical and chemical properties of Class G cement in oil well applications. In: 12th Int. Conf. on Fracture Mechanics of Concrete and Concrete Structures. Vienna, Austria.
Nguyen, V., Olayiwola, O., Guo, B., Liu, N., 2023. Well cement degradation and wellbore integrity in geological CO_2 storages: a literature review. arXiv 2301.02357.
Nochaiya, T., Wongkeo, W., Chaipanich, A., 2010. Utilization of fly ash with silica fume and properties of Portland cement–fly ash–silica fume concrete. Fuel 89, 768–774.
Noor, L., Tuinukuafe, A., Ideker, J.H., 2023. A critical review of the role of ettringite in binders composed of CAC–PC–C and CSA–PC–C. J. Am. Ceram. Soc. 106, 3303–3328.
Oldenburg, C.M., Jordan, P.D., Nicot, J.-P., Mazzoldi, A., Gupta, A.K., Bryant, S.L., 2011. Leakage risk assessment of the In Salah CO_2 storage project: applying the certification framework in a dynamic context. Energy Proc. 4, 4154–4161.
Onan, D., 1984. Effects of supercritical carbon dioxide on well cements. In: SPE Permian Basin Oil and Gas Recovery Conference.
Pacewska, B., Wilińska, I., Nowacka, M., 2011. Studies on the influence of different fly ashes and Portland cement on early hydration of calcium aluminate cement. J. Therm. Anal. Calorim. 106, 859–868.
Pan, Z., He, L., Qiu, L., Korayem, A.H., Li, G., Zhu, J.W., Collins, F., Li, D., Duan, W.H., Wang, M.C., 2015. Mechanical properties and microstructure of a graphene oxide–cement composite. Cem. Concr. Compos. 58, 140–147.
Panchmatia, P., Zhou, N.S., Juenger, M., van Oort, E., 2019. Monitoring the strength development of alkali-activated materials using an ultrasonic cement analyzer. J. Pet. Sci. Eng. 180, 538–544.
Papadakis, V.G., 1999. Effect of fly ash on Portland cement systems: part I. Low-calcium fly ash. Cem. Concr. Res. 29, 1727–1736.
Park, J.-G., Seo, D.-J., Lim, D.-Y., Lee, Y.-J., Heo, G.-H., 2023. A comparative study on electrical resistivity and compressive strength properties of cement composites incorporating conductive materials. Adv. Mater. Sci. Eng. 2023, 6676577.
Pearce, J., Khan, C., Golding, S., Rudolph, V., Underschultz, J., 2022. Geological storage of CO_2 and acid gases dissolved at surface in production water. J. Pet. Sci. Eng. 210, 110052.
Peng, Shudai, 2017. Overview of CO_2 Leakage Problems and Sealants for CO_2 Leakage Remediation (M.S. Thesis). Missouri University of Science & Technology, Rolla, Missouri, USA.
Plank, J., 2022. Cements for CO_2 capture and storage wells. In: Energy Transition: Climate Action and Circularity. ACS Publications, pp. 369–410.
Prakash, R., Mahgoub, S.A., Abedi, S., 2024. Chemo-mechanical alteration of silicate-rich shale rock after exposure to CO_2-rich brine at high temperature and pressure. Rock Mech. Rock Eng. 57, 5317–5333.
Puri, A., Voicu, G., Badanoiu, A., 2010. Expansive binders in the Portland cement–calcium aluminate cement–calcium sulfate system. Rev. Chim. (Bucharest) 61, 740–744.
Pyatina, T., Sugama, T., 2016. Acid resistance of calcium aluminate cement–fly ash F blends. Adv. Cem. Res. 28, 433–457.
Rasool, M.H., Ahmad, M., 2023. Reactivity of basaltic minerals for CO_2 sequestration via in situ mineralization: a review. Minerals 13, 1154.
Rasool, M.H., Ahmad, M., 2024. Revolutionizing shale drilling with potassium chloride-based natural deep eutectic solvent as an additive. J. Pet. Explor. Prod. Technol. 14, 85–105.
Rasool, M.H., Zamir, A., Elraies, K.A., Ahmad, M., Ayoub, M., Abbas, M.A., 2021. Potassium carbonate-based deep eutectic solvent (DES) as a potential drilling fluid additive in deep-water drilling applications. Pet. Sci. Technol. 39, 612–631.
Rasool, M.H., Ahmad, M., Ayoub, M., Zamir, A., Abbas, M.A., 2022. A review of the usage of deep eutectic solvents as shale inhibitors in drilling mud. J. Mol. Liq. 361, 119673.
Rasool, M.H., Ahmad, M., Ayoub, M., 2023a. Selecting geological formations for CO_2 storage: a comparative rating system. Sustainability 15, 6599.
Rasool, M.H., Ahmad, M., Siddiqui, N.A., Ali, H., 2024. Novel application of citric-acid-based natural deep eutectic solvent in drilling fluids for shale swelling prevention. Sci. Rep. 14, 25729.
Rasool, M.H., Ahmad, M., Siddiqui, N.A., Junejo, A.Z., 2023b. Eco-friendly drilling fluid: calcium chloride-based natural deep eutectic solvent (NADES) as an all-rounder additive. Energies 16, 5533.
Rasool, M.H., Ahmad, M., Siddiqui, N.A., Ridha, S., Khan, A., Ali, H., 2025. Mitigating shale swelling in deep drilling: novel natural deep eutectic solvent vs hybrid additives system. Deep Resour. Eng., 100173
Reales, O.A.M., Toledo Filho, R.D., 2017. A review on the chemical, mechanical and microstructural characterization of carbon nanotube–cement based composites. Constr. Build. Mater. 154, 697–710.
Recasens, M., Garcia, S., Mackay, E., Delgado, J., Maroto-Valer, M.M., 2017. Experimental study of wellbore integrity for CO_2 geological storage. Energy Proc. 114, 5249–5255.

Reddy, B.R., Zhang, J., Ellis, M., 2016. Cement strength retrogression issues in offshore deep-water applications—Do we know enough for safe cementing?. In: Proceedings of the Offshore Technology Conference Houston, Texas, USA.
Ribeiro, D., Agnelli, J., Morelli, M., 2013. Study of mechanical properties and durability of magnesium phosphate cement matrix containing grinding dust. Mater. Res. 16, 1113–1121.
Ribeiro, D., Paula, G., Morelli, M., 2019. Effect of boric acid content on the properties of magnesium phosphate cement. Constr. Build. Mater. 214, 557–564.
Ridha, S., Yerikania, U., 2014. Geopolymer cement slurries with enhanced mechanical and physical properties for oilwell cementing. In: Proceedings of the 5th Brunei International Conference on Engineering and Technology, Bandar Seri Begawan, Brunei. BICET Organizers.
Ridha, S., Yerikania, U., 2015. New nano-geopolymer cement system improves wellbore integrity upon acidizing job: experimental findings. In: Proceedings of the SPE/IATMI Asia Pacific Oil & Gas Conference and Exhibition, Nusa Dua. Bali, Indonesia.
Ridha, S., Jamali, M.F., Setiawan, R.A., 2017. Thickening time compatibility of geopolymer cement for drilling application. Appl. Mech. Mater. 864, 65–70.
Ridha, S., Abd Hamid, A.I., Che Ku Mazuan, C.K.A.H., 2018a. Influence of different brine water salinity on mechanical properties of fly ash-based geopolymer cement. Int. J. Struct. Integr. 9, 142–152.
Ridha, S., Abd Hamid, A.I., Setiawan, R.A., Shahari, A.R., 2018b. Influence of sulfuric and hydrochloric acid on the resistance of geopolymer cement with nanosilica additive for oil well cement application. Int. J. Struct. Integr. 9, 616–624.
Ridha, S., Setiawan, R.A., Pramana, A.A., Abdurrahman, M., 2020. Impact of wet supercritical CO_2 injection on fly ash geopolymer cement under elevated temperatures for well cement applications. J. Pet. Explor. Prod. Technol. 10, 243–247.
Rodrigues, E.C., de Andrade Silva, F., de Miranda, C.R., de Sa Cavalcante, G.M., de Souza Mendes, P.R., 2017. An appraisal of procedures to determine the flow curve of cement slurries. J. Pet. Sci. Eng. 159, 617–623.
Salah, I., 2010. Wellbore integrity at the Krechba Carbon Storage Site, In Salah, Algeria: 2. Reactive transport modeling of geochemical interactions near the cement–formation interface. In: Proceedings of the GHGT-10 Conference, vol. 4. Energy Procedia, pp. 5186–5194.
Salam, K., Arinkoola, A., Ajagbe, B., Sanni, O., 2013. Evaluation of thickening time of oil-field class G cement slurry at high temperature and pressure using experimental design. Int. J. Eng. Sci. 2, 361–367.
Samarakoon, M., Ranjith, P., Duan, W.H., Chen, B.K., Khandelwal, M., 2021. Early age properties of alkali-activated cement and Class G cement under different saturation conditions in oil well applications. Constr. Build. Mater. 271, 121543.
Samarakoon, M., Ranjith, P., Wanniarachchi, W., 2022. Properties of well cement following carbonated brine exposure under HTHP conditions: a comparative study of alkali-activated and Class G cements. Cem. Concr. Compos. 126, 104342.
Sanderson, R.A., Cann, G.M., Provis, J.L., 2017. Comparison of calorimetric methods for the assessment of slag cement hydration. Adv. Appl. Ceram. 116, 186–192.
Sedić, K., Ukrainczyk, N., Mandić, V., Gaurina-Međimurec, N., 2024. Carbonation study of new calcium aluminate cement-based CO_2 injection well sealants. Constr. Build. Mater. 419, 135517.
Shahidan, S., Aminuddin, E., Noor, K.M., Hannan, N.I.R.R., Bahari, N.A.S., 2017. Potential of hollow glass microsphere as cement replacement for lightweight foam concrete on thermal insulation performance. In: MATEC Web Conf., 103, 01014.
Shahriar, A., Nehdi, M.L., 2012. Rheological properties of oil well cement slurries. Proc. Inst. Civ. Eng. – Constr. Mater. 165, 25–44.
Shih, J.-Y., Chang, T.-P., Hsiao, T.-C., 2006. Effect of nanosilica on characterization of Portland cement composite. Mater. Sci. Eng. A 424, 266–274.
Silva, A.P., Segadães, A.M., Pinto, D.G., Oliveira, L.A., Devezas, T.C., 2012. Effect of particle size distribution and calcium aluminate cement on the rheological behaviour of all-alumina refractory castables. Powder Technol. 226, 107–113.
Singh, H., Islam, A., 2018. Enhanced safety of geologic CO_2 storage with nanoparticles. Int. J. Heat Mass Transf. 121, 463–476.
Skorpa, R., Todorovic, J., Torsæter, M., 2017. Porosity changes in mud-affected rock and cement upon reaction with CO_2. Energy Proc. 114, 5266–5274.
Smith, L., Billingham, M., Lee, C.H., Milanovic, D., Lunt, G., 2010. CO_2 sequestration wells – the lifetime integrity challenge. In: Abu Dhabi International Petroleum Exhibition and Conference. UAE, Abu Dhabi.
Sugama, T., 2006. Advanced Cements for Geothermal Wells. U.S. Department of Energy, Office of Geothermal Technologies.
Takase, K., Barhate, Y., Hashimoto, H., Lunkad, S.F., 2010. Cement-sheath wellbore integrity for CO_2 injection and storage wells. In: SPE Oil and Gas India Conference and Exhibition.
Tee, K.F., Mostofizadeh, S., 2021. A mini review on properties of Portland cement concrete with geopolymer materials as partial or entire replacement. Infrastructures 6, 26.
Teodoriu, C., Bello, O., 2020. A review of cement testing apparatus and methods under CO_2 environment and their impact on well integrity prediction – where do we stand? J. Pet. Sci. Eng. 187, 106736.
Tomić, L., Maričić, V.K., Danilović, D., Crnogorac, M., 2018. Criteria for CO_2 storage in geological formations. Podzemni radovi 32, 61–74.
Udebhulu, O.D., Aladeitan, Y., Azevedo, R.C., De Tomi, G., 2024. A review of cement sheath integrity evaluation techniques for carbon dioxide storage. J. Pet. Explor. Prod. Technol. 14, 1–23.
Vafaei, M., Allahverdi, A., 2016. Influence of calcium aluminate cement on geopolymerization of natural pozzolan. Constr. Build. Mater. 114, 290–296.
Verba, C., Montross, S., Spaulding, R., Dalton, L., Crandall, D., Moore, J., Glosser, D., Huerta, N., Kutchko, B., 2017. Foamed cement interactions with CO_2. In: NETL Technical Report Series. U.S. Department of Energy, National Energy Technology Laboratory, Morgantown, WV, USA.
Vieira, E.F., Cestari, A.R., da Silva, R.G., Pinto, A.A., Miranda, C.R., Conceição, A.C., 2004. Use of calorimetry to evaluate cement slurry resistance to the attack of acid solutions. Thermochim. Acta 419, 45–49.
Wagner, P., Ravi, K., Prohaska, M., 2021. Real-time monitoring of the effect of CO_2 on the cement sheath. In: Proceedings of the SPE Trinidad & Tobago Section Energy Resources Conference, Port of Spain, Trinidad and Tobago. Society of Petroleum Engineers.
Wang, D., Benzerzour, M., Hu, X., Huang, B., Chen, Z., Xu, X., 2020. Strength, permeability, and micromechanisms of industrial residue magnesium oxychloride cement solidified slurry. Int. J. GeoMech. 20, 04020088.
Wang, Y.-C., Lee, M.-G., Wang, W.-C., Kan, Y.-C., Kao, S.-H., Chang, H.-W., 2022. CO_2 curing on the mechanical properties of Portland cement concrete. Buildings 12, 817.
Wang, C., Chazallon, C., Braymand, S., Hornych, P., 2024. Thermogravimetric analysis (TGA) for characterization of self-cementation of recycled concrete aggregates in pavement. Thermochim. Acta 733, 179680.
Wang, C., Song, L., Liu, J., Wang, C., Wang, H., Xue, Z., Shi, A., 2025. Novel polymer development creates new high-temperature, high-pressure cement slurry suspending agent. SPE J. 1–16 (in press).
Wei, X., Tian, K., Xiao, L., 2010. Prediction of compressive strength of Portland cement paste based on electrical resistivity measurement. Adv. Cem. Res. 22, 165–170.
Wu, L., Wu, Z., Weng, L., Liu, Y., Chu, Z., Chen, J., 2024. Comparative analysis of polyacrylate latex-modified cement grout for water blocking and rock reinforcement with six alternative materials. Constr. Build. Mater. 429, 136377.
Xie, S., Qi, L., Zhou, D., 2004. Investigation of the effects of acid rain on the deterioration of cement concrete using accelerated tests established in laboratory. Atmos. Environ. 38, 4457–4466.
Xin, H., Zeng, J., Deng, Q., Wang, J., Shi, L., Zou, J., 2020. A novel calcium phosphate cement with good CO_2 and H_2S corrosion resistance. In: ISOPE International Ocean and Polar Engineering Conference.
Xu, L., Wu, K., Rößler, C., Wang, P., Ludwig, H., 2017. Influence of curing temperatures on the hydration of calcium aluminate cement/Portland cement/calcium sulfate blends. Cem. Concr. Compos. 80, 298–306.
Xu, B., Yuan, B., Wang, Y., Zeng, S., Yang, Y., 2019. Nanosilica-latex reduces carbonation-induced degradation in cement of CO_2 geological storage wells. J. Nat. Gas Sci. Eng. 65, 237–247.
Yamamoto, Y., 1972. Retarders for Concrete, and their Effects on setting-time and Shrinkage. PhD Dissertation. Purdue University, West Lafayette, Indiana, USA.
Yan, R., Wang, L., Ni, Y., Zhang, S., He, Z., Guan, B., 2024. A study on the properties of composite modified mortar with styrene–butadiene rubber latex and silica fume. Polymers 16, 697.
Yang, Z., Shi, X., Creighton, A.T., Peterson, M.M., 2009. Effect of styrene–butadiene rubber latex on the chloride permeability and microstructure of Portland cement mortar. Constr. Build. Mater. 23, 2283–2290.
Yang, J., Shi, Y., Yang, X., Liang, M., Li, Y., Li, Y., Ye, N., 2013. Durability of autoclaved construction materials of sewage sludge–cement–fly ash–furnace slag. Constr. Build. Mater. 48, 398–405.
Yang, Y., Liu, J., Wang, B., Liu, R., 2020. Properties of fly ash blended magnesium potassium phosphate cement cured in presence of sulfuric acid. Constr. Build. Mater. 244, 118349.
Yang, H., Wang, L., Yang, C., Zhao, J., Huang, G., Guo, Y., Liu, W.V., 2024. Mechanical performance of oil-well cement slurries cured and tested under high-temperatures and high-pressures for deep-well applications. Cem. Concr. Res. 175, 107355.
Yu, R., Spiesz, P., Brouwers, H., 2014. Effect of nano-silica on the hydration and microstructure development of ultra-high-performance concrete (UHPC) with a low binder amount. Constr. Build. Mater. 65, 140–150.
Yu, L., Wang, S., Qiao, Z., Xu, L., Wu, K., Li, P., Yang, Z., 2023. Effect of curing time and temperature on the mechanical properties of green and ultra-high-strength non-sintered aggregate via autoclave technology. Constr. Build. Mater. 374, 130874.
Zhang, M., Bachu, S., 2011. Review of integrity of existing wells in relation to CO_2 geological storage: what do we know? Int. J. Greenh. Gas Control 5, 826–840.
Zhang, B., Zou, C., Peng, Z., Zheng, Y., Zhang, J., 2020. Study on the preparation and anti-CO_2 corrosion performance of soap-free latex for oil well cement. ACS Omega 5, 23028–23038.
Zhang, S., Zhang, C., Pang, X., Shi, L., Song, M., Yu, B., Kong, X., 2024. Phase compositions and pore structure of phosphate-modified calcium aluminate cement

hardened pastes with varied dosages of sodium polyphosphate. Cem. Concr. Res. 184, 107609.
Zhao, R., Sanjayan, J.G., 2011. Geopolymer and Portland cement concretes in simulated fire. Mag. Concr. Res. 63, 163–173.
Zhao, L., Guo, X., Song, L., Song, Y., Dai, G., Liu, J., 2020. An intensive review on the role of graphene oxide in cement-based materials. Constr. Build. Mater. 241, 117939.
Zhao, F., Wang, C., Li, D., Chen, Z., 2024. A comprehensive review of CO_2 corrosion in oil well cement: mechanisms, determinants, and mitigation strategies. In: OMAE – International Conference on Offshore Mechanics and Arctic Engineering. ASME.
Živica, V., Bajza, A., 2001. Acidic attack of cement-based materials — a review. Part 1: principle of acidic attack. Constr. Build. Mater. 15, 331–340.